N73 22429

NASA TECHNICAL MEMORANDUM

NASA TM X- 68218

NASA TM X- 68218

THE PRELIMINARY DESIGN OF BEARINGS FOR THE CONTROL SYSTEM OF A HIGH-TEMPERATURE LITHIUM-COOLED NUCLEAR REACTOR

by H. G. Yacobucci, W. D. Waldron,
and J. A. Walowit
Lewis Research Center
Cleveland, Ohio 44135

April, 1973

ABSTRACT

The design of bearings for the control system of a fast reactor concept is presented. The bearings are required to operate at temperatures up to 2200° F in one of two fluids, lithium or argon. Basic bearing types are the same regardless of the fluid. Crowned cylindrical journals were selected for radially loaded bearings and modified spherical bearings were selected for bearings under combined thrust and radial loads. Graphite and aluminum oxide are the materials selected for the argon atmosphere bearings while cermet compositions (carbides or nitrides bonded with refractory metals) were selected for the lithium lubricated bearings. Mounting of components is by shrink fit or by axial clamping utilizing differential thermal expansion.

THE PRELIMINARY DESIGN OF BEARINGS FOR THE CONTROL SYSTEM OF A HIGH-TEMPERATURE LITHIUM-COOLED NUCLEAR REACTOR

by H. G. Yacobucci, W. D. Waldron,* and J. A. Walowit*

Lewis Research Center
National Aeronautics and Space Administration
Cleveland, Ohio

SUMMARY

This paper describes the designs of the bearings used to guide and support the fueled control drum system for a compact fast spectrum nuclear reactor concept. The bearings are required to operate for about 5 years at temperatures up to 2200° F in one of two fluids, lithium or argon. The bearing types selected are essentially the same for both fluids. Crowned cylindrical journals (rotating members) and cylindrical bearings (stationary members) were selected for those bearing sets subjected to pure radial loads. Spherical journals in modified spherical bearings were selected for those bearing sets supporting thrust as well as radial loads.

All bearings are designed to avoid loads near an edge. Since the load vector rotates during control drum movement, split bearing configurations were avoided to eliminate the possibility of the load vector passing over the bearing split line causing high edge loads and potential failure.

Aluminum oxide coated T-111 (T_s-8W-2H_f) and graphite were the materials selected for the argon atmosphere bearing sets. Potential candidate materials for the lithium environment bearing sets are cermets. Typical compositions are hafnium nitride, hafnium carbide, or zirconium carbide bonded with tungsten or molybdenum.

Graphite and aluminum oxide properties are well documented but the cermet properties were unknown and "best estimate" values had to be used in the designs.

Shrink fit type mounting methods are used to lock the bearings and journals in place. No mounting problems are anticipated over the entire operating temperature range for either the graphite bearings or the cermet journals mounted on TZM (Mo-0.5 Ti-0.08 Zr-0.02 C) shafts. The final dimensions of the cermet bearings mounted in T-111 housings and the cermet journal mounted on the T-111 shaft cannot be set until the thermal expan-

---

*W. D. Waldron and Dr. J. A. Walowit are employees of Mechanical Technology Incorporated (MTI), Latham, N.Y. The design work presented in this paper was done by MTI under subcontract to the General Electric Co. (G.E.), Cincinnati, Ohio. This work was part of a program conducted by G.E. for NASA under contract NAS3-13447.

sion coefficients of the cermets are known. However, once the coefficients are known a proper fit can be determined.

INTRODUCTION

The NASA Lewis Research Center has recently terminated work on a technology program for a compact, fast-spectrum nuclear reactor for space electric power generation. This report covers a part of the work performed under that program. Reference 1 describes the liquid-metal cooled reactor concept used to identify problems associated with advanced, high temperature reactors of this type. During the course of this study several reactivity control methods were considered. These were movable fuel, movable poison, and movable reflector.

The movable fuel method employing rotatable drums (see fig. 1) cooled by flowing lithium offers a large amount of reactivity control regardless of reactor size. However, it requires a moving lithium-to-gas seal and high temperature (up to 2200° F) bearings that operate in lithium or in an inert gas. The design of these bearings, which represents an important step in the development of this control system, is presented in this paper.

Each of the six control drums contains asymmetrically positioned fuel pins which are rotated into or out of the core to control the amount of reactivity. Rotational torque is transmitted to a control drum through the bellows-sealed rotary drive mechanism labeled "penetration device" in figure 1. Hermetic sealing is accomplished by a double bellows assembly through which passes a torque transmitting rotating rod as shown in figure 2. Argon gas, which is used to monitor the double bellows for leaks, occupies the space to the left of the bellows assembly in figure 2.

A schematic of the control drum and penetration device system with its nine bearing sets is shown in figure 3. Separation of the two fluids by the bellows assembly is not shown in figure 3 but bearing sets numbered 5, 6, and 9 are immersed in lithium while the rest operate in argon. Obviously, the environment and the high temperature requirement present difficult materials problems for this application.

Final verification of the materials selected for these bearings can only be accomplished through rigorous testing under simulated operating conditions but the bearing designs must be tailored to the materials characteristics. Graphite and aluminum oxide (Al_2O_3) were selected for the argon atmosphere bearings. These are the same materials chosen for the SNAP-8 and advanced ZrH reactors (ref. 2). The highly corrosive nature of lithium and elevated temperatures greatly limit the number of materials that could be used in the liquid metal (ref. 3).

Six cermet compositions were selected for development as candidate materials for the lithium lubricated bearings:

1. HfN + 10 w/o W

2. HfC + 10 w/o TaC + 10 w/o W

3. HfC + 10 w/o W

4. ZrC + 17 w/o W

5. HfC + 2 w/o NbC + 8 w/o Mo

6. HfN + 10 w/o TaN + 10 w/o W

A companion program (ref. 4) was initiated to determine the candidate cermet material properties, corrosion resistance and fabricability. However, the bearing design work was completed before the properties were obtained so all of the cermet properties used in this study are conservative "best estimate" values. It will be shown that satisfactory bearing designs can be accomplished as long as the properties fall within the assumed range of values. It is only the final dimensions of certain bearing components that cannot be exactly specified until properties such as thermal expansion coefficients are established.

BEARING DESIGN PHILOSOPHY

During the course of the bearing design work, several analyses were made of the control drum drive system to establish the maximum potential bearing loads and the nature of these loads. Also investigated were various methods of decelerating the drum, different bearing material friction coefficients, and the effect of bearing misalinement. The general approach was to first determine the maximum potential bearing loads, then to provide bearing designs that would support these loads within specified stress limits. Vibration loads during launch were neglected in this study. The reactor would probably be launched cold with solidifed lithium in the core. This should prevent relative motion between bearing components. If necessary mechanical locking devices could be employed to accomplish the same result.

For the bearings required to take thrust as well as radial loads, a spherical journal (rotating member) inside a modified spherical bearing (stationary member) were selected. Some ellipticity was introduced into the spherical bearing member to insure that the spherical journal did not contact the bearing lower edge under pure thrust load conditions. For the purely radial bearings, crowned cylindrical journals in cylindrical bearings were selected. Crowning of the journal together with proper selection of radial clearance provides misalignment capability and eliminates bearing edge loading which can lead to failure with the relatively brittle materials used in this application. Because the load vector rotates during control drum movement, split bearing configurations were avoided to eliminate the possibility of the load vector passing over the bearing split line which could also cause high edge loads.

The brittleness of the cermet materials also precluded the use of stress riser type fasteners such as keyed slots to mount the bearing components. The bearings are held in the T-111 housing members by simple interference fits. This is readily accomplished with the graphite bearings with no stress problems over the design temperature range (70^{o} to 2200^{o} F). The cermet bearings, on the other hand, do present a problem because the thermal expansion coefficient is not accurately known and it is not possible to design a fit to accommodate a range in coefficients from 3.5×10^{-6} to 4.0×10^{-6} in./in.-^{o}F which was assumed for design purposes. It is shown, however, that once the expansion coefficient is defined, an acceptable fit can be established.

Also, because of the low coefficient of thermal expansion for the TZM control drum shaft, the cermet journals grow away from the shaft with temperature. To insure that the journals do not move radially when load directions reverse, journals 6 and 9 are axially clamped by means of TZM tubes around the shaft. The clamping force is generated by the relative expansion of the cermet. Unlike the other cermet to refractory mounts, this concept is not stress limited over the assumed expansion coefficient and design temperature ranges.

Journal 5 is held on the T-111 nutating rod with the same axial clamp concept with a T-111 sleeve. However, in this case the axial clamping force decreases as the temperature increases. As is the case with the cermet bearings, once the expansion rate of the cermet is defined an acceptable fit can be established.

BEARING LOAD ANALYSIS

The reactor control drum is designed to rotate 180^{o} and may be stationary in any position within the 180^{o} arc. The two extreme positions (zero and 180^{o}) are defined as the "full-in" and "full-out" positions. A scram cycle is defined as the rotation of the control drum from any position to a "full-out" position (the position of minimum power). However, for design purposes a scram cycle was defined as the total 180^{o} rotation from a full-in to a full-out position. The specified period of the 180^{o} scram cycle was 0.4 second.

To accomplish a scram cycle, torque must be applied to accelerate the control drum to some prescribed velocity; then a reverse torque must be applied to decelerate the drum and bring it to rest at the end of the cycle. The maximum velocity during the scram cycle was specified at 15.7 rad/sec. Two acceleration rates, 49.1 and 58.8 rad/sec^{2} and two deceleration rates 196.4 and 118.0 rad/sec^{2} were considered in the design analysis.

The torque required to accelerate the control drum is delivered through the penetration device by means of an actuator which drives the input shaft supported on bearings 1 and 2 (see fig. 3). Different methods of decelerating the control drum were considered during the course of the

design effort. These methods included absorption of the deceleration torque through the penetration device and absorption by the use of a dashpot (see fig. 1).

The conceptual dashpot is a single vane rotary actuator with a shaped chamber which allows free vane rotation through the first 120° of travel. A decelerating torque is developed in the final 60° by a gradual reduction in the clearance between the vane and the chamber wall. The force acting on the vane causes a bearing reaction force which is dependent on the angular orientation of the vane with respect to the penetration device crankarm. In this study the two extreme vane orientations were used: (1) in-phase with the crankarm and (2) 180° out-of-phase with the crankarm. In addition to vane orientation, loads were also analyzed with the dashpot located above or below the control drum. The latter case has the dashpot and penetration device on the same end of the control drum as depicted in figure 1.

The loads on the control drum and penetration device journal bearings are derived from two sources. One source is the reaction of the torque required to accelerate and decelerate the control drum and the other is reaction of the friction torque in the bearings. Additional friction forces are generated by the misalinement of the control drum bearings (numbers 6 and 9), and the axis defined by bearings numbers 1 and 2. Noncoincidence of these two centerlines causes slipping to occur in bearings 7 and 8 plus rotation in bearings 3 and 5. The friction force produced by this slippage is independent of the magnitude of misalinement since magnitude affects only the distance of sliding travel.

Several load analyses were made in order to establish the maximum bearing loads for each of the scram cycles and to determine the most favorable location of the dashpot and orientation of its vane. A summary of the different load analyses that were performed is given in table I. The geometries and inertias assumed for these analyses are shown in figure 3 which depicts the entire rotating assembly comprised of the penetration device and the control drum. The coefficient of friction of all the graphite-aluminum oxide bearings was assumed to be 0.3. The other properties of the cermet and graphite bearing materials that were used in the design analyses are given in tables II and III. The properties of graphite are well documented but those of the cermets were unknown at the time of the design work; therefore, those properties shown in table II are "best estimate" values.

The results of the analyses of the forces on each bearing for the case where the acceleration and deceleration torque is supplied through the penetration device (case A per table I) are given in appendix A. The results for the analyses with the deceleration torque absorbed by a dashpot (case B per table I) are summarized in tables IV and V.

The analysis for Cases IB1 to IVB4 neglects misalinement and considers only the cermet bearings (numbers 5, 6, and 9) with the drive torque supplied by a reaction imposed perpendicular to the crankarm at

bearing 5. This simplification introduces some error in the absolute value of the bearing reactions but does not compromise the comparative conclusions since the primary result of the analysis was to establish the best location of the dashpot. Also, as is shown later, the maximum loads (which were used for design purposes) resulted from the analysis of Case IVA in which misalinement was considered.

The results of Cases IB1 to IVB4* lead to the conclusion that, if a dashpot is to be utilized to decelerate the control drum, it should be located below the control drum and out-of-phase with the crank arm (B4 cases). This will decrease the loads on the cermet bearings, particularly bearings 5 and 6, but more importantly, it will eliminate load reversals so that the journal does not slam through the clearance space at the point where the drum mode changes from acceleration to deceleration.**

The loads calculated by these analyses are conservative since they are calculated assuming the scram cycles consist of a constant acceleration then an instantaneous change to a constant deceleration. Also, the highest assumed coefficient of friction was used for the cermet. A summary of the maximum resultant bearing loads used for design purposes is given in table VI. For each assumed case there were four calculations made for each of the following conditions during the scram cycle: zero and maximum velocity while accelerating and maximum and zero velocity while decelerating. All the values in table VI are for a drum acceleration of 58.8 rad/sec^2 at the maximum velocity of 15.7 rad/sec and a cermet coefficient of friction of 0.7.

The maximum radial load of bearing number 4 is given as 340 pounds in table VI. This corresponds to a radial load of 680 pounds in Case IVA since the load is shared by two bearings in the gimbal design. Also, the maximum radial load at bearing number 6 is 500 pounds in table VI and 377 pounds in appendix A, Case IVA. This discrepancy is due to the fact that 500 pounds was used to size bearing number 6 early in the design phase and when the final analysis determined the maximum load to be 377 pounds, the bearing size was not changed.

BEARING DESIGN DETAILS

The details of the penetration device and control drum bearings are

---

*For B3 and B4 cases, the control drum span was increased by 2.0 inches to accommodate the dashpot.

**In the case of the bottom located dashpot with the vane in phase with the crank arm and engagement at 0.267 sec (Cases IIIB3 and IVB3), the radial load reversal is less than the 250 pound thrust load; thus violent motion through the clearance is not probable. However, in a zero g environment the thrust load is not present and adequate axial positioning is not maintained.

delineated in figure 2. All bearings except the two required to take an axial load (numbers 2 and 6) are made up of a straight cylindrical bearing member and a crowned cylindrical journal member. The crowned journals together with radial clearance permit accommodation of misalinement without imposing high bearing edge loads.

Thrust loads resulting from the weight of the control drum (on bearing 6) and the penetration device input shaft (on bearing 2) are taken on modified spherical combination journal-thrust bearings. The rotating journal member is spherical in shape while the stationary bearing member can be described as "football" shaped. This bearing geometry is shown schematically in figure 4.

It can be seen by examining figure 4 that if (e) were set at zero, the stationary bearing member would be a sphere and the journal would contact the bearing (with pure thrust load) at the lower edge resulting in excessive contact stresses and probable severe damage. This situation is prevented by making the bearing elliptical in shape (displacing the center of radius (R_B) a distance (e) from the center of rotation) which causes the line of contact to move up on the sphere. Since the minimum contact stress occurs when the contact is at 45° (see appendix B) from the centerline, the values of radial clearance (c), ellipticity (e), and radius (R_B) have been set to nominally achieve the 45° contact for bearings 2 and 6.

As radial load is applied to the combination journal-thrust bearings the contact changes from a uniform circumferential line at 45° to a partial circumferential line at an angle greater than 45°. As the contact point moves up the bearing surface (greater than 45°) the contact stress for a constant force vector increases as a result of the reduced member conformity. This can be seen in figure 4 where moving up the bearing surface causes R_2 to be greater than R_1. Since the contact stress is a function of R/R_S, larger values of R result in larger contact stress. The limiting case is that of zero thrust and pure radial load where the contact is at 90° and the stress is a maximum. These two bearings have been sized for this limiting maximum stress case (zero thrust load, maximum radial load).

The bearing size, geometry, and clearance relations were established to satisfy the following criteria.

1. Maximum Hertzian compressive stress less than 30 000 psi on cermet bearings and 20 000 psi on graphite bearings (tables II and III).

2. Maximum Hertzian shear stress less than 10 000 psi on cermet bearings and 6667 psi on graphite bearings. It should be noted that for frictionless Hertz contact the maximum stresses will be compressive. The maximum shear stress will occur below the surface at a value approximately 30 percent of the maximum compressive stress, thus the compressive stress criteria would dominate. However, when the coefficient of friction is greater than 0.3, the maximum shear stress occurs at the center of contact

of the surface and it can be shown to be very nearly equal to the coefficient of friction times the maximum Hertzian stress. In general, for the higher coefficients of friction under consideration for the cermet bearings ($\mu = 0.7$) the maximum allowable shear stress will be first to be reached. Hence the maximum allowable compressive stresses allowable to satisfy the above shear stress criteria are:

$$S_{c\ max} = \frac{S_{s\ max}}{\mu_{max}} = 14\ 300 \text{ psi (cermet) and } 22\ 200 \text{ psi (graphite)}$$

Since the value for graphite (assuming $\mu_{max} = 0.3$) exceeds the aforementioned compressive stress criteria (number 1), the 22 200 psi value is disregarded. The maximum allowable compressive stress for the cermet bearings becomes 14 300 psi because of the 0.7 value for μ_{max}.

3. Bearing diametral clearance larger than the maximum particle size of the powder used to fabricate the bearing material which is assumed to be 0.001 inch for the graphite and 0.004 inch for the cermet. This permits sufficient space for the strongest of the wear debris particles to be accommodated within the bearing confines without jamming.

4. Maximum area of contact angle of 120° for crowned journal bearings which is close to the limit of the applicability of the theory used to calculate the contact stresses.

5. A minimum distance equivalent to a third of the Hertzian contact area half width in the axial direction remaining between the bearing edge and the contact area. This is to provide adequate bearing edge structure as shown in figure 5.

As was indicated above, the details of the bearings are shown in figure 2. In addition the significant design parameters are indicated in table VII which summarizes the bearing size, geometry, clearance, design load (from table VI) maximum stress, contact angle, and misalinement tolerance.

The maximum compressive stress values given are for the design load case and maximum clearance conditions which result in minimum bearing conformity (highest stresses). In the case of the graphite bearings (1, 2, 3, 4, 7, and 8) the stress shown is for 2200° F where the modulus of elasticity is highest (see table III). In all cases, the compressive stresses are lower than those indicated in the aforementioned design criteria 1 and 2.

The circumferential extent of the contact area is based upon the minimum clearance cases where the conformity and contact area are the greatest. In all cases this value is less than 120°. Likewise the tolerance to misalinement is based upon the minimum clearance where the large contact area limits the axial misalinement.

It should be noted that for the crowned journal bearings, the allowable misalinements shown assume only one type at a time. For example, if the axial centerline of bearing number 1 is misalined by 0.191 inch, no angular misalinement is allowed because the axial extent of the contact area would fall outside of the 1/3 half width confine. This is not considered a problem however, since the magnitude of the tolerance misalinements are quite large. In the case of spherical bearings 2 and 6, the degree of misalinement is limited only by the reverse thrust bearing clearance.

As the design of the bearing evolved, the sizes and configurations changed. All of the load analyses conducted to establish the design loads were based upon the original bearing sizes and configurations. After completing the bearing designs described in this report, a load analysis duplicating the original analysis worst case conditions (Case IVA) was made using the final bearing geometries. The results are summarized on table VIII where it can be seen that, for all bearings, the final load values are lower than used for design purposes.

BEARING MOUNTING

Graphite Bearings (Numbers 1, 2, 3, 4, 7, and 8)

The graphite bearing pieces are held in the T-111 housings by means of a simple shrink fit. The expansion coefficient of the graphite is greater than that of T-111 (see fig. 6 and table III). Thus, the fit grows tighter with increased temperature. The low modulus of elasticity of the graphite readily accommodates the differential thermal expansion and the resulting thermal stresses are small. The assembly fits, room temperature, and 2200° F member stresses, and friction torque values are summarized in table IX. For all bearings except number 4, the minimum torque restraint is greater than the maximum bearing friction torque so that the bearing will not turn in the T-111 housing during operation. However, for bearing number 4, a pin is used to lock the bearing from turning.

Aluminum Oxide Journals (Numbers 1, 2, 3, 4, 7, and 8)

The aluminum oxide surface is plasma sprayed upon the T-111 base metal; therefore, no mechanical fasteners are involved with these bearing components.

Cermet Bearings (Numbers 5, 6, and 9)

All three cermet bearings are held in the T-111 housings by means of a cylindrical interference fit. This interference will change with a change in temperature depending on the expansion rates of the two materials. The coefficient of thermal expansion of T-111 and cermet is given

in figure 6. Although the cermet expansion rate has not been measured at this time, it is expected to be in the range of 3.5×10^{-6} in./in. $^{\circ}$F to 4.0×10^{-6} in./in. $^{\circ}$F. Hence the design is based on accommodating any rate in this range. As can be seen from examining figure 6, if the thermal expansion rate of the cermet is 4.0×10^{-6} in./in. $^{\circ}$F, the amount of interference will increase as the temperature is increased throughout the temperature range of zero degrees to 2200° F. However, if the thermal expansion rate of the cermet is 3.5×10^{-6} in./in. $^{\circ}$F, the amount of interference will increase with increased temperature up to 975° F and then decrease with increasing temperature from 975° to 2200° F. This situation makes it impossible for one interference fit to meet all the design criteria for all assumed cermet expansion rates.

A design that meets all design criteria, i.e., a tight fit and all members within design stress limits throughout the operating temperature range, is possible with a known value of cermet expansion rate between 3.5×10^{-6} to 4.0×10^{-6} in./in. $^{\circ}$F. The amount of room temperature interference for all three bearings as a function of cermet expansion rate is shown in figure 7.

Cermet Journals (Numbers 6 and 9)

Since the thermal expansion coefficient of TZM (see fig. 6) is in all cases lower than the assumed expansion of the cermet (3.5×10^{-6} to 4.0×10^{-6} in./in. $^{\circ}$F) the journal member grows away from the shaft. The magnitude of growth precludes the use of an interference fit at assembly of sufficient magnitude to insure a tight fit at 2200° F because the room temperature tensile stress in the cermet would exceed the 10 000 psi design limit. In the design shown in figure 2, the journal is assembled loose on the shaft and incorporates an axial clamping tube on the shaft which generates enough force over the 450° F to 2200° F operating range to maintain the radial position of the journal member by friction between the end of the clamp tube and cermet journal. This clamping force is generated by the axial growth of the cermet journal with themperature. The clamping force and resultant significant stresses imposed on the bearing and shaft members are summarized in table X. The clamping forces shown are sufficient to locate the bearing radially and maintain its position during a load reversal equivalent to the design load assuming the friction coefficient between the cermet and TZM is in excess of 0.55. Although the force is also sufficient to prevent rotation of the journal on the shaft, a polygon spline is provided as a back-up antirotation device.

As can be seen from table X, the clamping force decreases with increasing temperature for the low cermet expansion rates and increases with increasing temperature for the high cermet expansion rates. This is explained by examining figure 6 (thermal coefficient of expansion of TZM and cermets) and the fact that the cermet expansion rate was assumed to remain constant throughout the temperature range. By examining figure 6,

it is evident that there is a substantial difference between the expansion rates at 450° F regardless of the assumed cermet rate. However, at 2200° F there is very little difference between TZM and the 3.5×10^{-6} cermet rate but a substantial difference between TZM and 4.0×10^{-6}. Thus, as can be seen from table X the clamping forces at 2200° F is less than those at 450° F for the cermet expansion rates of 3.5×10^{-6} in./in. °F. However, for cermet expansion rates of 4.0×10^{-6} in./in. °F, the clamping forces increase with increasing temperatures.

Cermet Journal (Number 5)

The mounting design of journal number 5, is shown in figure 2. This design of the cermet journal on the T-111 nutating rod utilizes the same "axial clamp" concept that is used in mounting journals 6 and 9. However, there is a basic difference since the internal member in this case is T-111 whereas it was TZM for journals 6 and 9. Because the internal member is T-111 the axial clamp does not always get tighter with increasing temperature, as was the case with journals 6 and 9. In fact, the axial clamping force will decrease with increasing temperature for any cermet expansion rate below 3.95×10^{-6} in./in. °F.

As was the case with the cylindrical fit of the cermet bearings, it is not possible to have one interference fit accommodate all cermet expansion rates. However, once the cermet expansion rate is known, a design with sufficient clamping force and acceptable stresses in all members is possible.

The proper initial interference at room temperature for various cermet expansion rates are given in table XI. Also tabulated in table XI is the minimum axial clamping forces and the stresses in all three members at 70°, 450°, and 2200° F. The stress in the T-111 post is a tensile stress while the T-111 sleeve and cermet journal are in compression.

SUMMARY OF RESULTS

The bearings in the control drum and penetration device system are designed for operation at temperatures up to 2200° F in one of two fluids, lithium or argon. The basic bearing types selected are the same for each fluid. Bearing sets subjected to pure radial loads consist of crowned cylindrical journals (rotating members) mated with cylindrical bearings (stationary members). For the bearing sets required to take thrust as well as radial loads, a spherical journal inside of a modified spherical bearing was selected.

The crowned and the spherical configurations provide for a substantial amount of misalinement between the control drum shaft and the penetration device input shaft. Furthermore, these configurations lend themselves to elimination of edge loads which must be avoided with the relatively brittle materials being contemplated for this application. The

edge loading problem also precluded split bearing designs since the load vector rotates through as much as 180^{o}.

Graphite and aluminum oxide are the materials selected for the bearing sets operating in argon. Six candidate cermet compositions were selected for the lithium lubricated bearings. These compositions consist of ceramics (primarily hafnium nitride, hafnium carbide, or zirconium carbide) bonded with tungsten or molybdenum.

Mounting of the cermet bearings presents some problems because of the brittleness of the material and because of the unknown coefficients of thermal expansion. Stress riser type fasteners such as keyed slots or fasteners that could put tension loads on the cermets were avoided. Simple interference fits are used to hold the bearings in the T-111 housing members. A range of coefficients of expansion was assumed for design purposes and although it is not possible to design a fit to accommodate the entire range, it is shown that once the coefficient is known, a proper fit can be established.

The cermet journals are held on their shafts by means of axial clamps which rely on differential thermal expansion for their clamping forces. When the shaft material is TZM there is no problem because the low TZM expansion coefficient causes increasing clamping pressure with increasing temperature. However, for the cermet journal mounted on the T-111 nutating rod, the clamping pressure decreases with increasing temperature. For this case, the expansion coefficient must be known before the room temperature fit can be established which will provide the proper clamping pressure over the entire operating temperature range.

The graphite bearings present no obvious mounting problems over the entire operating temperature range and since their journals consist of an aluminum oxide coating on a T-111 shaft there is no mechanical fastener involved.

If the control drum is to be decelerated during a scram by means of a single vane rotary dashpot, the dashpot and the penetration device should be located on the same end of the control drum. Furthermore, the vane of the dashpot should be oriented 180^{o} out-of-phase with the penetration device crank arm. This not only reduces cermet bearing loads (compared to deceleration through the penetration device) but also prevents the cermet journals from slamming through the clearance space at the point in time where the control drum mode changes from acceleration to deceleration.

APPENDIX A

PENETRATION DEVICE AND CONTROL DRUM BEARING LOADS FOR ACCELERATION AND DECELERATION FORCES PROVIDED BY ACTUATOR

Figure 8 shows the penetration device shafts as free bodies with the various force and moment vectors indicated by arrows. The angle between the nutating shaft (Body C) and the control drum centerline is α. The equilibrium force and moment equations for the various bodies are:

Body A

$\Sigma FX, \quad FX1 + FX2 - FX7 - FX8 = 0$

$\Sigma FY, \quad FY1 + FY2 + FW7(\sin \alpha) + FWB(\sin \alpha) = FV7(\cos \alpha) + FV8(\cos \alpha)$

$\Sigma FZ, \quad FZ2 - FW7(\cos \alpha) - FW8(\cos \alpha) = FV7(\sin \alpha) + FV8(\sin \alpha)$

$\Sigma MX, \quad FY2(LZ2) - FW7(\cos \alpha)(LY7) + FW8(\cos \alpha)(LY8) + FW7(\sin \alpha)(LZ7)$

$+ FW8(\sin \alpha)(LZ8) = FV7(\cos \alpha)(LZ7) + FV8(\cos \alpha)(LZ8)$

$+ FV7(\sin \alpha)(LY7) - FV8(\sin \alpha)(LY8)$

$\Sigma MY, \quad -FX2(LZ2) + FX7(LZ7) + FX8(LZ8) - MV7(\cos \alpha) - MV8(\cos \alpha) = 0$

$\Sigma MZ, \quad T + FX7 - FX8(LY8) - MV7(\sin \alpha) - MV8(\sin \alpha) = -MZ1 - MZ2$

Body B

$\Sigma FV, \quad FV3 = FV7 + FV8$

$\Sigma FW, \quad FW3 = FW7 + FW8$

$\Sigma FX, \quad FX7 + FX8 - FX3 = 0$

$\Sigma MV, \quad MV7 + MV8 = MV3$

$\Sigma MW, \quad -FX7(LY7)/(\cos \alpha) + FX8(LY8)/(\cos \alpha) - FX3(LY3)/(\cos \alpha) = MW3$

Body C

$\Sigma FV, \quad FV3 + FY4(\cos \alpha) + FZ4(\sin \alpha) - FV5 = -FVB$

$\Sigma FW, \quad FZ4(\cos \alpha) - FY4(\sin \alpha) = -FWB - FW3 + FW5$

$\Sigma FX, \quad FX3 + FX4 - FX5 = 0$

$\Sigma MV, \quad FX3(LR) + MZ4(\sin \alpha) + FX5(LR) = -MV3 - MY4(\cos \alpha) + MV5$

$\Sigma MW, \quad MZ4(\cos \alpha) = -MW3 + MY4(\sin \alpha) + MW5$

$\Sigma MX, \quad -FV3(LR) - FV5(LR) = -FVB(LB) - MXB - MX3 - MX4 + MX5$

Body D

$\Sigma FX, \quad FX5 + FX6 + FX9 = -FXD$

$\Sigma FY, \quad FV5(\cos \alpha) + FY6 + FY9 = -FYD + FW5(\sin \alpha)$

$\Sigma FZ, \quad FV5(\sin \alpha) + FZ6 = -FZD - FW5(\cos \alpha) - WTD$

$\Sigma MX, \quad -FV5(\cos \alpha)(LZ5) + FV5(\sin \alpha)(LY5) - FY6(LZ6) = FYD(LD) - MX5$

$\quad - FW5(\sin \alpha)(LZ5) - FW5(\cos \alpha)(LY5)$

$\Sigma MY, \quad FX5(LZ5) + FX6(LZ6) = -FXD(LD) - MV5(\cos \alpha) + MW5(\sin \alpha)$

$\quad + WTD(LOD)$

$\Sigma MZ, \quad -FX5(LY5) = -MZD - MZ6 - MZ9 - MW5(\cos \alpha) - MV5(\sin \alpha)$

A computer program was used to solve the above sets of simultaneous equations for various friction and acceleration conditions. The results of these calculations are presented in the remaining pages of this appendix.

NUTATING ROD FORCE ANALYSIS

CASE 3 ACCEL 49.1 RAD/SEC2, OMEG=0

LZ2	LZ3	LZ7	LZ8	LR	LB
6.300	9.693	8.413	9.243	6.250	5.375

LZ5	LZ6	LD
32.700	30.850	15.500

LY3	LY5	LY7	LY8	L0D	WTD
1.880	1.880	2.170	0.450	0.670	250.000

FVB	FWB	MXB	FYD	FXD	FZD	MZD
-38.400	88.500	149.000	0.000	0.000	-26.000	-129.000

MU1	MU2	MU6	MU9	MU3	MU5
0.300	0.300	0.300	0.300	0.300	0.300

MU04	MUI4	MUB3	MUB5	MU78	MUT6
0.300	0.300	0.300	0.300	0.300	0.300

R1	R2	R6	R9	R3	R5
0.375	0.437	0.437	0.437	0.312	0.312

R04	RI4	RB3	RB5	R78	RT6
1.000	0.687	0.500	0.500	0.312	0.700

ZERO FRICTION LOADS

FY1	FX1	MZ1	FY2	FX2	FZ2
0.000	-36.988	0.000	0.000	105.605	0.000

MZ2	FV3	FX3	FW3	MV3	MX3
0.000	0.000	68.617	0.000	0.000	0.000

MW3	FY4	FX4	FZ4	MY4	MX4
0.000	54.484	-137.234	-75.613	0.000	0.000

MZ4	FV5	FX5	FW5	MV5	MX5
0.000	-9.184	-68.617	0.000	0.000	0.000

MW5	FY6	FX6	FZ6	MZ6	FV7
0.000	9.116	78.161	-221.237	0.000	0.000

FX7	FW7	MV7	FV8	FX8	FW8
-37.451	0.000	0.000	0.000	106.068	0.000

MV8	FY9	FX9	MZ9	T
0.000	-.357	-9.544	0.000	129.000

CASE 3 ACCEL 49.1 RAD/SEC2, OMEG=0

WITH FRICTION, BEARINGS PERFECTLY ALIGNED

FY1	FX1	MZ1	FY2	FX2	FZ2
0.000	-65.673	-7.388	0.000	186.499	0.000
MZ2	FV3	FX3	FW3	MV3	MX3
-24.450	0.000	120.825	0.000	0.000	0.000
MW3	FY4	FX4	FZ4	MY4	MX4
11.309	54.484	-228.458	-75.613	-72.194	0.000
MZ4	FV5	FX5	FW5	MV5	MX5
-45.230	-9.184	-107.633	0.000	0.000	0.000
MW5	FY6	FX6	FZ6	MZ6	FV7
-10.111	9.116	119.418	-221.237	-62.161	0.000
FX7	FW7	MV7	FV8	FX8	FW8
-70.063	0.000	0.000	0.000	190.889	0.000
MV8	FY9	FX9	MZ9	T	
0.000	-.357	-11.785	-1.546	269.775	

WITH FRICTION, BEARINGS MISALIGNED

FY1	FX1	MZ1	FY2	FX2	FZ2
-20.164	-71.671	-8.376	92.028	199.785	56.941
MZ2	FV3	FX3	FW3	MV3	MX3
-28.837	85.664	128.114	32.688	-14.022	-9.724
MW3	FY4	FX4	FZ4	MY4	MX4
10.199	-117.472	-237.397	-130.567	-81.280	-36.198
MZ4	FV5	FX5	FW5	MV5	MX5
-46.800	-104.042	-109.283	32.004	12.076	11.544
MW5	FY6	FX6	FZ6	MZ6	FV7
-9.985	115.705	120.796	-223.225	-68.806	23.003
FX7	FW7	MV7	FV8	FX8	FW8
-73.637	-21.380	-7.011	62.661	201.751	54.068
MV8	FY9	FX9	MZ9	T	
-7.011	-6.854	-11.512	-1.757	283.575	

STOP
CP: 17.7 SEC I/O: 24.7 SEC

READY

NUTROD 15:06 FRIDAY 08/07/70

NUTATING ROD FORCE ANALYSIS

CASE 3 ACCEL 49.1 RAD/SEC2, OMEG=15.7 RAD/SEC

LZ2	LZ3	LZ7	LZ8	LR	LB
6.300	9.693	8.413	9.243	6.250	5.375

LZ5	LZ6	LD
32.700	30.850	15.500

LY3	LY5	LY7	LY8	LOD	WTD
1.880	1.880	2.170	0.450	0.670	250.000

FVB	FWB	MXB	FYD	FXD	FZD	MZD
-38.400	7.200	149.000	0.000	107.000	-26.000	-129.000

MU1	MU2	MU6	MU9	MU3	MU5
0.300	0.300	0.300	0.300	0.300	0.300

MU04	MUI4	MUB3	MUB5	MU78	MUT6
0.300	0.300	0.300	0.300	0.300	0.300

R1	R2	R6	R9	R3	R5
0.375	0.437	0.437	0.437	0.312	0.312

R04	RI4	RB3	RB5	R78	RT6
1.000	0.687	0.500	0.500	0.312	0.700

ZERO FRICTION LOADS

FY1	FX1	MZ1	FY2	FX2	FZ2
0.000	-36.988	0.000	0.000	105.605	0.000

MZ2	FV3	FX3	FW3	MV3	MX3
0.000	0.000	68.617	0.000	0.000	0.000

MW3	FY4	FX4	FZ4	MY4	MX4
0.000	30.029	-137.234	1.922	0.000	0.000

MZ4	FV5	FX5	FW5	MV5	MX5
0.000	-9.184	-68.617	0.000	0.000	0.000

MW5	FY6	FX6	FZ6	MZ6	FV7
0.000	9.116	24.401	-221.237	0.000	0.000

FX7	FW7	MV7	FV8	FX8	FW8
-37.451	0.000	0.000	0.000	106.068	0.000

MV8	FY9	FX9	MZ9	T
0.000	-.357	-62.734	0.000	129.000

CASE 3 ACCEL 49.1 RAD/SEC2, OMEG=15.7 RAD/SEC

WITH FRICTION, BEARINGS PERFECTLY ALIGNED

FY1	FX1	MZ1	FY2	FX2	FZ2
0.000	-65.309	-7.347	0.000	185.465	0.000
MZ2	FV3	FX3	FW3	MV3	MX3
-24.314	0.000	120.155	0.000	0.000	0.000
MW3	FY4	FX4	FZ4	MY4	MX4
11.247	30.029	-227.769	1.922	-68.333	0.000
MZ4	FV5	FX5	FW5	MV5	MX5
-43.946	-9.184	-107.613	0.000	0.000	0.000
MW5	FY6	FX6	FZ6	MZ6	FV7
-10.109	9.116	65.638	-221.237	-55.148	0.000
FX7	FW7	MV7	FV8	FX8	FW8
-69.675	0.000	0.000	0.000	189.830	0.000
MV8	FY9	FX9	MZ9	T	
0.000	-.357	-65.024	-8.525	268.279	

WITH FRICTION, BEARINGS MISALIGNED

FY1	FX1	MZ1	FY2	FX2	FZ2
-20.162	-71.664	-8.375	92.019	199.765	56.935
MZ2	FV3	FX3	FW3	MV3	MX3
-28.834	85.655	128.101	32.684	-14.020	-9.723
MW3	FY4	FX4	FZ4	MY4	MX4
10.198	-141.136	-238.683	-52.698	-73.329	-31.050
MZ4	FV5	FX5	FW5	MV5	MX5
-44.316	-103.196	-110.582	32.081	12.211	11.461
MW5	FY6	FX6	FZ6	MZ6	FV7
-10.009	114.891	68.408	-223.553	-64.476	23.001
FX7	FW7	MV7	FV8	FX8	FW8
-73.630	-21.378	-7.010	62.655	201.731	54.062
MV8	FY9	FX9	MZ9	T	
-7.010	-6.825	-64.826	-8.546	283.547	

STOP
CP: 18.2 SEC I/O: 36.5 SEC

READY

NUTATING ROD FORCE ANALYSIS

CASE 1 DECEL 196.4 RAD/SEC2, OMEG 15.7 RAD/SED

LZ2	LZ3	LZ7	LZ8	LR	LB
6.300	9.693	8.413	9.243	6.250	5.375

LZ5	LZ6	LD
32.700	30.850	15.500

LY3	LY5	LY7	LY8	LOD	WTD
1.880	1.880	2.170	0.450	0.670	250.000

FVB	FWB	MXB	FYD	FXD	FZD	MZD
-38.400	7.200	149.000	0.000	107.000	-26.000	517.000

MU1	MU2	MU6	MU9	MU3	MU5
0.300	0.300	0.300	0.300	0.300	0.300

MU24	MU14	MUB3	MUB5	MU78	MUT6
0.300	0.300	0.300	0.300	0.300	0.300

R1	R2	R6	R9	R3	R5
0.375	0.437	0.437	0.437	0.312	0.312

R24	R14	RB3	RB5	R78	RT6
1.000	0.687	0.500	0.500	0.312	0.700

ZERO FRICTION LOADS

FY1	FX1	MZ1	FY2	FX2	FZ2
0.000	148.239	0.000	0.000	-423.239	0.000

MZ2	FV3	FX3	FW3	MV3	MX3
0.000	0.000	-275.000	0.000	0.000	0.000

MW3	FY4	FX4	FZ4	MY4	MX4
0.000	30.029	550.000	1.922	0.000	0.000

MZ4	FV5	FX5	FW5	MV5	MX5
0.000	-9.184	275.000	0.000	0.000	0.000

MW5	FY6	FX6	FZ6	MZ6	FV7
0.000	9.116	-339.822	-221.237	0.000	0.000

FX7	FW7	MV7	FV8	FX8	FW8
150.095	0.000	0.000	0.000	-425.095	0.000

MV8	FY9	FX9	MZ9	T
0.000	-.357	-42.178	0.000	-517.000

CASE 1 DECEL 196.4 RAD/SEC2, ØMEG 15.7 RAD/SED

WITH FRICTION, BEARINGS PERFECTLY ALIGNED

FY1	FX1	MZ1	FY2	FX2	FZ2
0.000	104.052	-11.706	0.000	-298.701	0.000
MZ2	FV3	FX3	FW3	MV3	MX3
-39.160	0.000	-194.649	0.000	0.000	0.000
MW3	FY4	FX4	FZ4	MY4	MX4
18.219	30.029	411.980	1.922	-123.595	0.000
MZ4	FV5	FX5	FW5	MV5	MX5
-79.436	-9.184	217.331	0.000	0.000	0.000
MW5	FY6	FX6	FZ6	MZ6	FV7
-20.360	9.116	-278.893	-221.237	-83.042	0.000
FX7	FW7	MV7	FV8	FX8	FW8
99.608	0.000	0.000	0.000	-294.257	0.000
MV8	FY9	FX9	MZ9	T	
0.000	-.357	-45.438	-5.957	-297.699	

WITH FRICTION, BEARINGS MISALIGNED

FY1	FX1	MZ1	FY2	FX2	FZ2
-27.416	97.887	-11.436	127.365	-286.589	81.230
MZ2	FV3	FX3	FW3	MV3	MX3
-41.115	119.754	-188.702	47.403	-20.634	-13.659
MW3	FY4	FX4	FZ4	MY4	MX4
14.790	-212.232	406.888	-66.416	-123.682	-45.833
MZ4	FV5	FX5	FW5	MV5	MX5
-72.545	-141.026	218.186	55.103	23.865	16.057
MW5	FY6	FX6	FZ6	MZ6	FV7
-17.192	161.267	-280.506	-234.130	-91.586	30.710
FX7	FW7	MV7	FV8	FX8	FW8
97.610	-30.845	-10.317	89.044	-286.312	78.248
MV8	FY9	FX9	MZ9	T	
-10.317	-10.197	-44.680	-6.008	-294.309	

STØP
CP: 18.2 SEC I/O: 29.7 SEC

READY

NUTATING ROD FORCE ANALYSIS

CASE 1 DECEL 196.4 RAD/SEC2 , ONEG=0 RAD/SEC

LZ2	LZ3	LZ7	LZ8	LR	LB
6.300	9.693	8.413	9.243	6.250	5.375

LZ5	LZ6	LD
32.700	30.850	15.500

LY3	LY5	LY7	LY8	LOD	WTD
1.880	1.880	2.170	0.450	0.670	250.000

FVB	FWB	MXB	FYD	FXD	FZD	MZD
-38.400	88.500	149.000	0.000	0.000	-26.000	517.000

MU1	MU2	MU6	MU9	MU3	MU5
0.300	0.300	0.300	0.300	0.300	0.300

MU04	MUI4	MUB3	MUB5	MU78	MUT6
0.300	0.300	0.300	0.300	0.300	0.300

R1	R2	R6	R9	R3	R5
0.375	0.437	0.437	0.437	0.312	0.312

R04	RI4	RB3	RB5	R78	RT6
1.000	0.687	0.500	0.500	0.312	0.700

ZERO FRICTION LOADS

FY1	FX1	MZ1	FY2	FX2	FZ2
0.000	148.239	0.000	0.000	-423.239	0.000

MZ2	FV3	FX3	FW3	MV3	MX3
0.000	0.000	-275.000	0.000	0.000	0.000

MW3	FY4	FX4	FZ4	MY4	MX4
0.000	54.484	550.000	-75.613	0.000	0.000

MZ4	FV5	FX5	FW5	MV5	MX5
0.000	-9.184	275.000	0.000	0.000	0.000

MW5	FY6	FX6	FZ6	MZ6	FV7
0.000	9.116	-286.062	-221.237	0.000	0.000

FX7	FW7	MV7	FV8	FX8	FW8
150.095	0.000	0.000	0.000	-425.095	0.000

MV8	FY9	FX9	MZ9	T
0.000	-.357	11.062	0.000	-517.000

CASE 1 DECEL 196.4 RAD/SEC2 , OMEG=0 RAD/SEC

WITH FRICTION, BEARINGS PERFECTLY ALIGNED

FY1	FX1	MZ1	FY2	FX2	FZ2
0.000	106.590	-11.991	0.000	-305.988	0.000
MZ2	FV3	FX3	FW3	MV3	MX3
-40.115	0.000	-199.398	0.000	0.000	0.000
MW3	FY4	FX4	FZ4	MY4	MX4
18.664	54.484	422.389	-75.613	-128.731	0.000
MZ4	FV5	FX5	FW5	MV5	MX5
-82.077	-9.184	222.991	0.000	0.000	0.000
MW5	FY6	FX6	FZ6	MZ6	FV7
-20.890	9.116	-231.137	-221.237	-76.786	0.000
FX7	FW7	MV7	FV8	FX8	FW8
102.038	0.000	0.000	0.000	-301.436	0.000
MV8	FY9	FX9	MZ9	T	
0.000	-.357	8.146	-1.069	-304.962	

WITH FRICTION, BEARINGS MISALIGNED

FY1	FX1	MZ1	FY2	FX2	FZ2
-27.894	99.594	-11.636	129.586	-291.588	82.647
MZ2	FV3	FX3	FW3	MV3	MX3
-41.832	121.843	-191.993	48.230	-20.993	-13.897
MW3	FY4	FX4	FZ4	MY4	MX4
15.048	-192.541	415.022	-145.078	-131.895	-49.687
MZ4	FV5	FX5	FW5	MV5	MX5
-75.794	-143.821	223.029	56.287	24.394	16.379
MW5	FY6	FX6	FZ6	MZ6	FV7
-17.562	164.498	-231.899	-234.419	-86.502	31.246
FX7	FW7	MV7	FV8	FX8	FW8
99.313	-31.383	-10.497	90.597	-291.306	79.612
MV8	FY9	FX9	MZ9	T	
-10.497	-10.406	8.870	-1.793	-299.444	

STOP
CP: 17.5 SEC I/O: 24.7 SEC

READY

NUTATING ROD FORCE ANALYSIS

CASE 4 ACCEL 49.1 RAD/SEC2, OMEG=0

LZ2	LZ3	LZ7	LZ8	LR	LB
6.300	9.693	8.413	9.243	6.250	5.375

LZ5	LZ6	LD
32.700	30.850	15.500

LY3	LY5	LY7	LY8	LOD	WTD
1.680	1.880	2.170	0.450	0.670	250.000

FVB	FWB	MXB	FYD	FXD	FZD	MZD
-38.400	88.500	149.000	0.000	0.000	-26.000	-129.000

MU1	MU2	MU6	MU9	MU3	MU5
0.300	0.300	0.700	0.700	0.300	0.700

MU34	MUI4	MUB3	MUB5	MU78	MUT6
0.300	0.300	0.300	0.700	0.300	0.700

R1	R2	R6	R9	R3	R5
0.375	0.437	0.437	0.437	0.312	0.312

R04	RI4	RB3	RB5	R78	RT6
1.000	0.687	0.500	0.500	0.312	0.700

ZERO FRICTION LOADS

FY1	FX1	MZ1	FY2	FX2	FZ2
0.000	-36.988	0.000	0.000	105.605	0.000

MZ2	FV3	FX3	FW3	MV3	MX3
0.000	0.000	68.617	0.000	0.000	0.000

MW3	FY4	FX4	FZ4	MY4	MX4
0.000	54.484	-137.234	-75.613	0.000	0.000

MZ4	FV5	FX5	FW5	MV5	MX5
0.000	-9.184	-68.617	0.000	0.000	0.000

MW5	FY6	FX6	FZ6	MZ6	FV7
0.000	9.116	78.161	-221.237	0.000	0.000

FX7	FW7	MV7	FV8	FX8	FW8
-37.451	0.000	0.000	0.000	106.068	0.000

MV8	FY9	FX9	MZ9	T
0.000	-.357	-9.544	0.000	129.000

CASE 4 ACCEL 49.1 RAD/SEC2, ØMEG=0

WITH FRICTIØN, BEARINGS PERFECTLY ALIGNED

FY1	FX1	MZ1	FY2	FX2	FZ2
0.000	-110.730	-12.457	0.000	314.450	0.000
MZ2	FV3	FX3	FW3	MV3	MX3
-41.224	0.000	203.720	0.000	0.000	0.000
MW3	FY4	FX4	FZ4	MY4	MX4
19.068	54.484	-384.746	-75.613	-117.632	0.000
MZ4	FV5	FX5	FW5	MV5	MX5
-98.605	-9.184	-181.025	0.000	0.000	0.000
MW5	FY6	FX6	FZ6	MZ6	FV7
-39.587	9.116	196.924	-221.237	-168.710	0.000
FX7	FW7	MV7	FV8	FX8	FW8
-118.132	0.000	0.000	0.000	321.852	0.000
MV8	FY9	FX9	MZ9	T	
0.000	-.357	-15.899	-4.865	454.860	

WITH FRICTIØN, BEARINGS MISALIGNED

FY1	FX1	MZ1	FY2	FX2	FZ2
-42.696	-151.760	-17.736	194.864	423.032	120.570
MZ2	FV3	FX3	FW3	MV3	MX3
-61.061	181.388	271.273	69.214	-29.690	-20.589
MW3	FY4	FX4	FZ4	MY4	MX4
21.595	-341.770	-497.738	-110.679	-152.968	-74.040
MZ4	FV5	FX5	FW5	MV5	MX5
-121.588	-216.246	-226.465	154.967	67.903	65.831
MW5	FY6	FX6	FZ6	MZ6	FV7
-48.350	275.183	242.904	-306.742	-262.585	48.708
FX7	FW7	MV7	FV8	FX8	FW8
-155.922	-45.272	-14.845	132.681	427.195	114.486
MV8	FY9	FX9	MZ9	T	
-14.845	-22.339	-16.440	-8.484	600.453	

STØP
CP: 22.2 SEC I/O: 30.6 SEC

READY

NUTROD 14:55 FRIDAY 08/07/70

NUTATING ROD FORCE ANALYSIS

CASE 4 ACCEL 49.1 RAD/SEC2, OMEG=15.7 RAD/SEC

LZ2	LZ3	LZ7	LZ8	LR	LB
6.300	9.693	8.413	9.243	6.250	5.375

LZS	LZ6	LD
32.700	30.850	15.500

LY3	LY5	LY7	LY8	L0D	WTD
1.880	1.880	2.170	0.450	0.670	250.000

FVB	FWB	MXB	FYD	FXD	FZD	MZD
-38.400	7.200	149.000	0.000	107.000	-26.000	-129.000

MU1	MU2	MU6	MU9	MU3	MU5
0.300	0.300	0.700	0.700	0.300	0.700

MU04	MUI4	MUB3	MUB5	MU78	MUT6
0.300	0.300	0.300	0.700	0.300	0.700

R1	R2	R6	R9	R3	R5
0.375	0.437	0.437	0.437	0.312	0.312

R04	RI4	RB3	RB5	R78	RT6
1.000	0.687	0.500	0.500	0.312	0.700

ZERO FRICTION LOADS

FY1	FX1	MZ1	FY2	FX2	FZ2
0.000	-36.988	0.000	0.000	105.605	0.000

MZ2	FV3	FX3	FW3	MV3	MX3
0.000	0.000	68.617	0.000	0.000	0.000

MW3	FY4	FX4	FZ4	MY4	MX4
0.000	30.029	-137.234	1.922	0.000	0.000

MZ4	FV5	FX5	FW5	MV5	MX5
0.000	-9.184	-68.617	0.000	0.000	0.000

MW5	FY6	FX6	FZ6	MZ6	FV7
0.000	9.116	24.401	-221.237	0.000	0.000

FX7	FW7	MV7	FV8	FX8	FW8
-37.451	0.000	0.000	0.000	106.068	0.000

MV8	FY9	FX9	MZ9	T
0.000	-.357	-62.784	0.000	129.000

CASE 4 ACCEL 49.1 RAD/SEC2, OMEG=15.7 RAD/SEC

WITH FRICTION, BEARINGS PERFECTLY ALIGNED

FY1	FX1	MZ1	FY2	FX2	FZ2
0.000	-110.455	-12.426	0.000	313.668	0.000
MZ2	FV3	FX3	FW3	MV3	MX3
-41.122	0.000	203.214	0.000	0.000	0.000
MW3	FY4	FX4	FZ4	MY4	MX4
19.021	30.029	-384.137	1.922	-115.243	0.000
MZ4	FV5	FX5	FW5	MV5	MX5
-97.778	-9.184	-180.923	0.000	0.000	0.000
MW5	FY6	FX6	FZ6	MZ6	FV7
-39.565	9.116	143.056	-221.237	-152.256	0.000
FX7	FW7	MV7	FV8	FX8	FW8
-117.838	0.000	0.000	0.000	321.052	0.000
MV8	FY9	FX9	MZ9	T	
0.000	-.357	-69.133	-21.148	453.729	

WITH FRICTION, BEARINGS MISALIGNED

FY1	FX1	MZ1	FY2	FX2	FZ2
-43.239	-153.691	-17.961	197.344	428.416	122.104
MZ2	FV3	FX3	FW3	MV3	MX3
-61.838	183.696	274.725	70.095	-30.068	-20.851
MW3	FY4	FX4	FZ4	MY4	MX4
21.870	-371.649	-504.583	-33.445	-151.707	-76.906
MZ4	FV5	FX5	FW5	MV5	MX5
-122.206	-219.201	-229.858	157.191	68.907	66.746
MW5	FY6	FX6	FZ6	MZ6	FV7
-49.044	278.985	192.704	-307.975	-254.629	49.328
FX7	FW7	MV7	FV8	FX8	FW8
-157.906	-45.848	-15.034	134.369	432.631	115.942
MV8	FY9	FX9	MZ9	T	
-15.034	-22.653	-69.845	-22.461	608.094	

STOP
CP: 22.2 SEC I/O: 36.7 SEC

READY

NUTROD 14:40 FRIDAY 08/07/70

NUTATING ROD FORCE ANALYSIS

CASE 2 196.4 RAD/SEC2, OMEG 15.7 RAD/SEC

LZ2	LZ3	LZ7	LZ8	LR	LB
6.300	9.693	8.413	9.243	6.250	5.375

LZ5	LZ6	LD
32.700	30.850	15.500

LY3	LY5	LY7	LY8	LOD	WTD
1.880	1.880	2.170	0.450	0.670	250.000

FVB	FWB	MXB	FYD	FXD	FZD	MZD
-38.400	7.200	149.000	0.000	107.000	-26.000	517.000

MU1	MU2	MU6	MU9	MU3	MU5
0.300	0.300	0.700	0.700	0.300	0.700

MU04	MU14	MUB3	MUB5	MU78	MUT6
0.300	0.300	0.300	0.700	0.300	0.700

R1	R2	R6	R9	R3	R5
0.375	0.437	0.437	0.437	0.312	0.312

R04	RI4	RB3	RB5	R78	RT6
1.000	0.687	0.500	0.500	0.312	0.700

ZERO FRICTION LOADS

FY1	FX1	MZ1	FY2	FX2	FZ2
0.000	148.239	0.000	0.000	-423.239	0.000

MZ2	FV3	FX3	FW3	MV3	MX3
0.000	0.000	-275.000	0.000	0.000	0.000

MW3	FY4	FX4	FZ4	MY4	MX4
0.000	30.029	550.000	1.922	0.000	0.000

MZ4	FV5	FX5	FW5	MV5	MX5
0.000	-9.184	275.000	0.000	0.000	0.000

MW5	FY6	FX6	FZ6	MZ6	FV7
0.000	9.116	-339.822	-221.237	0.000	0.000

FX7	FW7	MV7	FV8	FX8	FW8
150.095	0.000	0.000	0.000	-425.095	0.000

MV8	FY9	FX9	MZ9	T
0.000	-.357	-42.178	0.000	-517.000

CASE 2 196.4 RAD/SEC2, OMEG 15.7 RAD/SEC

WITH FRICTION, BEARINGS PERFECTLY ALIGNED

FY1	FX1	MZ1	FY2	FX2	FZ2
0.000	74.637	-8.397	0.000	-214.260	0.000
MZ2	FV3	FX3	FW3	MV3	MX3
-28.089	0.000	-139.623	0.000	0.000	0.000
MW3	FY4	FX4	FZ4	MY4	MX4
13.069	30.029	296.565	1.922	-88.971	0.000
MZ4	FV5	FX5	FW5	MV5	MX5
-77.767	-9.184	156.942	0.000	0.000	0.000
MW5	FY6	FX6	FZ6	MZ6	FV7
-34.335	9.116	-215.019	-221.237	-174.240	0.000
FX7	FW7	MV7	FV8	FX8	FW8
71.449	0.000	0.000	0.000	-211.072	0.000
MV8	FY9	FX9	MZ9	T	
0.000	-.357	-48.923	-14.966	-213.542	

WITH FRICTION, BEARINGS MISALIGNED

FY1	FX1	MZ1	FY2	FX2	FZ2
-17.877	63.828	-7.457	83.049	-186.873	52.966
MZ2	FV3	FX3	FW3	MV3	MX3
-26.809	78.086	-123.045	30.910	-13.454	-8.906
MW3	FY4	FX4	FZ4	MY4	MX4
9.644	-147.015	270.528	5.784	-81.177	-30.323
MZ4	FV5	FX5	FW5	MV5	MX5
-64.455	-98.781	147.483	87.848	42.478	32.711
MW5	FY6	FX6	FZ6	MZ6	FV7
-27.409	132.219	-206.238	-278.066	-211.192	20.025
FX7	FW7	MV7	FV8	FX8	FW8
63.648	-20.112	-6.727	58.062	-186.693	51.022
MV8	FY9	FX9	MZ9	T	
-6.727	-11.589	-48.245	-15.178	-191.908	

STOP
CP: 18.7 SEC I/O: 32.1 SEC

READY

NUTROD 16:56 FRIDAY 08/07/70

NUTATING ROD FORCE ANALYSIS

CASE 2 DECEL 196.4 RAD/SEC2, OMEG=0 RAD/SEC

LZ2	LZ3	LZ7	LZ8	LR	LB
6.300	9.693	8.413	9.243	6.250	5.375

LZ5	LZ6	LD
32.700	30.850	15.500

LY3	LY5	LY7	LY8	LOD	WTD
1.880	1.880	2.170	0.450	0.670	250.000

FVB	FWB	MXB	FYD	FXD	FZD	MZD
-38.400	88.500	149.000	0.000	0.000	-26.000	517.000

MU1	MU2	MU6	MU9	MU3	MU5
0.300	0.300	0.700	0.700	0.300	0.700

MU84	MUI4	MUB3	MUB5	MU78	MUT6
0.300	0.300	0.300	0.700	0.300	0.700

R1	R2	R6	R9	R3	R5
0.375	0.437	0.437	0.437	0.312	0.312

R84	RI4	RB3	RB5	R78	RT6
1.000	0.687	0.500	0.500	0.312	0.700

ZERO FRICTION LOADS

FY1	FX1	MZ1	FY2	FX2	FZ2
0.000	148.239	0.000	0.000	-423.239	0.000

MZ2	FV3	FX3	FW3	MV3	MX3
0.000	0.000	-275.000	0.000	0.000	0.000

MW3	FY4	FX4	FZ4	MY4	MX4
0.000	54.484	550.000	-75.613	0.000	0.000

MZ4	FV5	FX5	FW5	MV5	MX5
0.000	-9.184	275.000	0.000	0.000	0.000

MW5	FY6	FX6	FZ6	MZ6	FV7
0.000	9.116	-286.062	-221.237	0.000	0.000

FX7	FW7	MV7	FV8	FX8	FW8
150.095	0.000	0.000	0.000	-425.095	0.000

MV8	FY9	FX9	MZ9	T
0.000	-.357	11.062	0.000	-517.000

CASE 2 DECEL 196.4 RAD/SEC2, OMEG=0 RAD/SEC

WITH FRICTION, BEARINGS PERFECTLY ALIGNED

FY1	FX1	MZ1	FY2	FX2	FZ2
0.000	80.293	-9.033	0.000	-230.497	0.000
MZ2	FV3	FX3	FW3	MV3	MX3
-30.218	0.000	-150.204	0.000	0.000	0.000
MW3	FY4	FX4	FZ4	MY4	MX4
14.059	54.484	319.512	-75.613	-98.501	0.000
MZ4	FV5	FX5	FW5	MV5	MX5
-84.640	-9.184	169.308	0.000	0.000	0.000
MW5	FY6	FX6	FZ6	MZ6	FV7
-37.031	9.116	-174.392	-221.237	-161.826	0.000
FX7	FW7	MV7	FV8	FX8	FW8
76.864	0.000	0.000	0.000	-227.068	0.000
MV8	FY9	FX9	MZ9	T	
0.000	-.357	5.085	-1.559	-229.724	

WITH FRICTION, BEARINGS MISALIGNED

FY1	FX1	MZ1	FY2	FX2	FZ2
-18.973	67.742	-7.914	88.143	-198.333	56.215
MZ2	FV3	FX3	FW3	MV3	MX3
-28.454	82.876	-130.591	32.805	-14.279	-9.452
MW3	FY4	FX4	FZ4	MY4	MX4
10.235	-133.239	287.595	-71.467	-88.903	-31.161
MZ4	FV5	FX5	FW5	MV5	MX5
-69.272	-104.090	157.004	93.227	45.184	34.577
MW5	FY6	FX6	FZ6	MZ6	FV7
-29.087	139.577	-162.670	-281.599	-203.551	21.253
FX7	FW7	MV7	FV8	FX8	FW8
67.551	-21.346	-7.140	61.622	-198.142	54.151
MV8	FY9	FX9	MZ9	T	
-7.140	-12.265	5.666	-4.133	-203.677	

STOP
CP: 19.4 SEC I/O: 26.3 SEC

READY

NUTROD 16:02 FRIDAY 06/07/70

NUTATING ROD FORCE ANALYSIS

CASE 3 ACCEL 58.8 RAD/SEC2, OMEG=0

LZ2	LZ3	LZ7	LZ8	LR	LB
6.300	9.693	8.413	9.243	6.250	5.375

LZ5	LZ6	LD
32.700	30.850	15.500

LY3	LY5	LY7	LY8	LOD	WTD
1.880	1.880	2.170	0.450	0.670	250.000

FVB	FWB	MXB	FYD	FXD	FZD	MZD
-38.400	88.500	149.000	0.000	0.000	-26.000	-155.000

MU1	MU2	MU6	MU9	MU3	MU5
0.300	0.300	0.300	0.300	0.300	0.300

MUO4	MUI4	MUB3	MUB5	MU78	MUT6
0.300	0.300	0.300	0.300	0.300	0.300

R1	R2	R6	R9	R3	R5
0.375	0.437	0.437	0.437	0.312	0.312

RO4	RI4	RB3	RB5	R78	RT6
1.000	0.687	0.500	0.500	0.312	0.700

ZERO FRICTION LOADS

FY1	FX1	MZ1	FY2	FX2	FZ2
0.000	-44.443	0.000	0.000	126.690	0.000

MZ2	FV3	FX3	FW3	MV3	MX3
0.000	0.000	82.447	0.000	0.000	0.000

MW3	FY4	FX4	FZ4	MY4	MX4
0.000	54.484	-164.894	-75.613	0.000	0.000

MZ4	FV5	FX5	FW5	MV5	MX5
0.000	-9.184	-82.447	0.000	0.000	0.000

MW5	FY6	FX6	FZ6	MZ6	FV7
0.000	9.116	92.820	-221.237	0.000	0.000

FX7	FW7	MV7	FV8	FX8	FW8
-45.000	0.000	0.000	0.000	127.446	0.000

MV8	FY9	FX9	MZ9	T
0.000	-.357	-10.374	0.000	155.000

CASE 3 ACCEL 58.8 RAD/SEC2, OMEG=0

WITH FRICTION, BEARINGS PERFECTLY ALIGNED

FY1	FX1	MZ1	FY2	FX2	FZ2
0.000	-75.223	-8.463	0.000	213.619	0.000
MZ2	FV3	FX3	FW3	MV3	MX3
-28.005	0.000	138.396	0.000	0.000	0.000
MW3	FY4	FX4	FZ4	MY4	MX4
12.954	54.484	-261.836	-75.613	-81.761	0.000
MZ4	FV5	FX5	FW5	MV5	MX5
-51.519	-9.184	-123.440	0.000	0.000	0.000
MW5	FY6	FX6	FZ6	MZ6	FV7
-11.586	9.116	136.159	-221.237	-64.350	0.000
FX7	FW7	MV7	FV8	FX8	FW8
-80.252	0.000	0.000	0.000	218.647	0.000
MV8	FY9	FX9	MZ9	T	
0.000	-.357	-12.719	-1.668	309.006	

WITH FRICTION, BEARINGS MISALIGNED

FY1	FX1	MZ1	FY2	FX2	FZ2
-23.059	-81.960	-9.578	105.239	228.465	65.115
MZ2	FV3	FX3	FW3	MV3	MX3
-32.977	97.961	146.505	37.380	-16.035	-11.119
MW3	FY4	FX4	FZ4	MY4	MX4
11.663	-142.007	-271.718	-138.586	-91.506	-40.895
MZ4	FV5	FX5	FW5	MV5	MX5
-53.008	-117.555	-125.213	36.428	13.829	13.052
MW5	FY6	FX6	FZ6	MZ6	FV7
-11.365	130.834	137.613	-223.380	-71.803	26.306
FX7	FW7	MV7	FV8	FX8	FW8
-84.208	-24.449	-8.017	71.656	230.713	61.829
MV8	FY9	FX9	MZ9	T	
-8.017	-7.765	-12.400	-1.918	324.283	

STOP
CP: 17.6 SEC I/O: 28.3 SEC

READY

NUTROD 10:39 WEDNESDAY 07/01/70

NUTATING ROD FORCE ANALYSIS

CASE 3 ACCEL 58.8 RAD/SEC2, OMEG=15.7 RAD/SEC

LZ2	LZ3	LZ7	LZ8	LR	LB
6.300	9.693	8.413	9.243	6.250	5.375

LZ5	LZ6	LD
32.700	30.850	15.500

LY3	LY5	LY7	LY8	LOD	WTD
1.880	1.880	2.170	0.450	0.670	250.000

FVB	FWB	MXB	FYD	FXD	FZD	MZD
-38.400	88.500	149.000	0.000	107.000	-26.000	-155.000

MU1	MU2	MU6	MU9	MU3	MU5	MU4
0.300	0.300	0.300	0.300	0.300	0.300	0.300

MUB3	MUB5	MU7	MU8
0.300	0.300	0.300	0.300

R1	R2	R6	R9	R3	R5
0.375	0.437	0.437	0.437	0.312	0.312

R04	RI4	RB3	RB5	R78	RT6
1.000	0.687	0.500	0.500	0.312	0.700

ZERO FRICTION LOADS

FY1	FX1	MZ1	FY2	FX2	FZ2
0.000	-44.443	0.000	0.000	126.890	0.000

MZ2	FV3	FX3	FW3	MV3	MX3
0.000	0.000	82.447	0.000	0.000	0.000

MW3	FY4	FX4	FZ4	MY4	MX4
0.000	54.484	-164.894	-75.613	0.000	0.000

MZ4	FV5	FX5	FW5	MV5	MX5
0.000	-9.184	-82.447	0.000	0.000	0.000

MW5	FY6	FX6	FZ6	MZ6	FV7
0.000	9.116	39.060	-221.237	0.000	0.000

FX7	FW7	MV7	FV8	FX8	FW8
-45.000	0.000	0.000	0.000	127.446	0.000

MV8	FY9	FX9	MZ9	T
0.000	-.357	-63.614	0.000	155.000

CASE 3 ACCEL 58.8 RAD/SEC2, ØMEG=15.7 RAD/SEC

WITH FRICTIØN, BEARINGS PERFECTLY ALIGNED

FY1	FX1	MZ1	FY2	FX2	FZ2
0.000	-75.224	-8.463	0.000	213.620	0.000
MZ2	FV3	FX3	FW3	MV3	MX3
-28.038	0.000	138.396	0.000	0.000	0.000
MW3	FY4	FX4	FZ4	MY4	MX4
12.975	54.484	-261.834	-75.613	-81.760	0.000
MZ4	FV5	FX5	FW5	MV5	MX5
-51.560	-9.184	-123.439	0.000	0.000	0.000
MW5	FY6	FX6	FZ6	MZ6	FV7
-11.604	9.116	82.397	-221.237	-57.340	0.000
FX7	FW7	MV7	FV8	FX8	FW8
-80.259	0.000	0.000	0.000	218.655	0.000
MV8	FY9	FX9	MZ9	T	
0.000	-.357	-65.959	-8.657	309.058	

WITH FRICTION, BEARINGS MISALIGNED

FY1	FX1	MZ1	FY2	FX2	FZ2
-23.313	-82.859	-9.684	106.398	230.970	65.831
MZ2	FV3	FX3	FW3	MV3	MX3
-33.377	99.039	148.111	37.790	-16.210	-11.242
MW3	FY4	FX4	FZ4	MY4	MX4
11.810	-144.158	-274.713	-139.289	-92.402	-41.314
MZ4	FV5	FX5	FW5	MV5	MX5
-53.590	-118.741	-126.602	36.815	13.982	13.184
MW5	FY6	FX6	FZ6	MZ6	FV7
-11.505	132.161	85.318	-223.392	-67.559	26.596
FX7	FW7	MV7	FV8	FX8	FW8
-85.138	-24.718	-8.105	72.444	233.249	62.508
MV8	FY9	FX9	MZ9	T	
-8.105	-7.845	-65.717	-8.687	327.895	

STØP
CP: 17.9 SEC I/Ø: 41.1 SEC

READY

NUTATING ROD FORCE ANALYSIS

CASE 1 DECEL 118 RAD/SEC2, OMEG=15.7 RAD/SEC

LZ2	LZ3	LZ7	LZ8	LR	LB
6.300	9.693	8.413	9.243	6.250	5.375

LZ5	LZ6	LD
32.700	30.850	15.500

LY3	LY5	LY7	LY8	LOD	WTD
1.880	1.880	2.170	0.450	0.670	250.000

FVB	FWB	MXB	FYD	FXD	FZD	MZD
-38.400	88.500	149.000	0.000	107.000	-26.000	310.000

MU1	MU2	MU6	MU9	MU3	MU5	MU4
0.300	0.300	0.300	0.300	0.300	0.300	0.300

MUB3	MUB5	MU7	MU8
0.300	0.300	0.300	0.300

R1	R2	R6	R9	R3	R5
0.375	0.437	0.437	0.437	0.312	0.312

R04	R14	RB3	RB5	R78	RT6
1.000	0.687	0.500	0.500	0.312	0.700

ZERO FRICTION LOADS

FY1	FX1	MZ1	FY2	FX2	FZ2
0.000	88.886	0.000	0.000	-253.780	0.000

MZ2	FV3	FX3	FW3	MV3	MX3
0.000	0.000	-164.894	0.000	0.000	0.000

MW3	FY4	FX4	FZ4	MY4	MX4
0.000	54.484	329.787	-75.613	0.000	0.000

MZ4	FV5	FX5	FW5	MV5	MX5
0.000	-9.184	164.894	0.000	0.000	0.000

MW5	FY6	FX6	FZ6	MZ6	FV7
0.000	9.116	-223.113	-221.237	0.000	0.000

FX7	FW7	MV7	FV8	FX8	FW8
89.999	0.000	0.000	0.000	-254.893	0.000

MV8	FY9	FX9	MZ9	T
0.000	-.357	-48.781	0.000	-310.000

CASE 1 DECEL 118 RAD/SEC2, ØMEG=15.7 RAD/SEC

WITH FRICTION, BEARINGS PERFECTLY ALIGNED

FY1	FX1	MZ1	FY2	FX2	FZ2
0.000	56.531	-6.360	0.000	-162.285	0.000
MZ2	FV3	FX3	FW3	MV3	MX3
-21.300	0.000	-105.754	0.000	0.000	0.000
MW3	FY4	FX4	FZ4	MY4	MX4
9.914	54.484	224.494	-75.613	-71.066	0.000
MZ4	FV5	FX5	FW5	MV5	MX5
-44.518	-9.184	118.741	0.000	0.000	0.000
MW5	FY6	FX6	FZ6	MZ6	FV7
-11.165	9.116	-174.301	-221.237	-69.368	0.000
FX7	FW7	MV7	FV8	FX8	FW8
54.112	0.000	0.000	0.000	-159.866	0.000
MV8	FY9	FX9	MZ9	T	
0.000	-.357	-51.440	-6.752	-161.702	

WITH FRICTION, BEARINGS MISALIGNED

FY1	FX1	MZ1	FY2	FX2	FZ2
-14.810	52.882	-6.178	68.805	-154.827	43.883
MZ2	FV3	FX3	FW3	MV3	MX3
-22.237	64.694	-101.945	25.609	-11.147	-7.379
MW3	FY4	FX4	FZ4	MY4	MX4
8.003	-77.207	221.121	-111.953	-74.354	-28.028
MZ4	FV5	FX5	FW5	MV5	MX5
-41.859	-81.012	119.176	30.564	13.048	9.182
MW5	FY6	FX6	FZ6	MZ6	FV7
-9.551	92.228	-175.150	-228.781	-74.025	16.590
FX7	FW7	MV7	FV8	FX8	FW8
52.728	-16.664	-5.574	48.104	-154.673	42.273
MV8	FY9	FX9	MZ9	T	
-5.574	-5.773	-51.026	-6.740	-158.961	

STØP
CP: 19.1 SEC I/O: 34.0 SEC

READY

CASE IIIA

NUTATING ROD FORCE ANALYSIS

CASE 1 DECEL 118 RAD/SEC2, OMEG=0 RAD/SEC

LZ2	LZ3	LZ7	LZ8	LR	LB
6.300	9.693	8.413	9.243	6.250	5.375

LZ5	LZ6	LD
32.700	30.850	15.500

LY3	LY5	LY7	LY8	LOD	WTD
1.680	1.880	2.170	0.450	0.670	250.000

FVB	FWB	MXB	FYD	FXD	FZD	MZD
-38.400	88.500	149.000	0.000	0.000	-26.000	310.000

MU1	MU2	MU6	MU9	MU3	MU5
0.300	0.300	0.300	0.300	0.300	0.300

MU04	MUI4	MUB3	MUB5	MU78	MUT6
0.300	0.300	0.300	0.300	0.300	0.300

R1	R2	R6	R9	R3	R5
0.375	0.437	0.437	0.437	0.312	0.312

R04	RI4	RB3	RB5	R78	RT6
1.000	0.687	0.500	0.500	0.312	0.700

ZERO FRICTION LOADS

FY1	FX1	MZ1	FY2	FX2	FZ2
0.000	88.886	0.000	0.000	-253.780	0.000

MZ2	FV3	FX3	FW3	MV3	MX3
0.000	0.000	-164.894	0.000	0.000	0.000

MW3	FY4	FX4	FZ4	MY4	MX4
0.000	54.484	329.787	-75.613	0.000	0.000

MZ4	FV5	FX5	FW5	MV5	MX5
0.000	-9.184	164.894	0.000	0.000	0.000

MW5	FY6	FX6	FZ6	MZ6	FV7
0.000	9.116	-169.352	-221.237	0.000	0.000

FX7	FW7	MV7	FV8	FX8	FW8
89.999	0.000	0.000	0.000	-254.893	0.000

MV8	FY9	FX9	MZ9	T
0.000	-.357	4.459	0.000	-310.000

CASE 1 DECEL 118 RAD/SEC2, OMEG=0 RAD/SEC

WITH FRICTION, BEARINGS PERFECTLY ALIGNED

FY1	FX1	MZ1	FY2	FX2	FZ2
0.000	59.624	-6.708	0.000	-171.161	0.000
MZ2	FV3	FX3	FW3	MV3	MX3
-22.439	0.000	-111.537	0.000	0.000	0.000
MW3	FY4	FX4	FZ4	MY4	MX4
10.440	54.484	236.701	-75.613	-74.545	0.000
MZ4	FV5	FX5	FW5	MV5	MX5
-46.776	-9.184	125.164	0.000	0.000	0.000
MW5	FY6	FX6	FZ6	MZ6	FV7
-11.747	9.116	-127.354	-221.237	-63.199	0.000
FX7	FW7	MV7	FV8	FX8	FW8
57.077	0.000	0.000	0.000	-168.614	0.000
MV8	FY9	FX9	MZ9	T	
0.000	-.357	2.191	-.291	-170.587	

WITH FRICTION, BEARINGS MISALIGNED

FY1	FX1	MZ1	FY2	FX2	FZ2
-15.526	55.437	-6.477	72.131	-162.305	46.003
MZ2	FV3	FX3	FW3	MV3	MX3
-23.285	67.820	-106.868	26.846	-11.685	-7.735
MW3	FY4	FX4	FZ4	MY4	MX4
8.376	-83.495	231.710	-113.764	-77.440	-29.084
MZ4	FV5	FX5	FW5	MV5	MX5
-43.665	-84.427	124.842	31.966	13.667	9.574
MW5	FY6	FX6	FZ6	MZ6	FV7
-9.973	96.158	-127.419	-229.090	-69.036	17.392
FX7	FW7	MV7	FV8	FX8	FW8
55.280	-17.468	-5.843	50.428	-162.148	44.314
MV8	FY9	FX9	MZ9	T	
-5.843	-6.026	2.577	-.859	-166.677	

STOP
CP: 19.1 SEC I/O: 26.7 SEC

READY

NUTROD 16:13 FRIDAY 08/07/70

NUTATING ROD FORCE ANALYSIS

CASE 4 ACCEL 58.8 RAD/SEC2, OMEG=0

LZ2	LZ3	LZ7	LZ8	LR	LB
6.300	9.693	8.413	9.243	6.250	5.375

LZ5	LZ6	LD
32.700	30.850	15.500

LY3	LY5	LY7	LY8	LOD	WTD
1.880	1.880	2.170	0.450	0.670	250.000

FVB	FWB	MXB	FYD	FXD	FZD	MZD
-38.400	88.500	149.000	0.000	0.000	-26.000	-155.000

MU1	MU2	MU6	MU9	MU3	MU5
0.300	0.300	0.700	0.700	0.300	0.700

MU04	MUI4	MUB3	MUB5	MU78	MUT6
0.300	0.300	0.300	0.700	0.300	0.700

R1	R2	R6	R9	R3	R5
0.375	0.437	0.437	0.437	0.312	0.312

R04	RI4	RB3	RB5	R78	RT6
1.000	0.687	0.500	0.500	0.312	0.700

ZERO FRICTION LOADS

FY1	FX1	MZ1	FY2	FX2	FZ2
0.000	-44.443	0.000	0.000	126.890	0.000

MZ2	FV3	FX3	FW3	MV3	MX3
0.000	0.000	82.447	0.000	0.000	0.000

MW3	FY4	FX4	FZ4	MY4	MX4
0.000	54.484	-164.894	-75.613	0.000	0.000

MZ4	FV5	FX5	FW5	MV5	MX5
0.000	-9.184	-82.447	0.000	0.000	0.000

MW5	FY6	FX6	FZ6	MZ6	FV7
0.000	9.116	92.820	-221.237	0.000	0.000

FX7	FW7	MV7	FV8	FX8	FW8
-45.000	0.000	0.000	0.000	127.446	0.000

MV8	FY9	FX9	MZ9	T
0.000	-.357	-10.374	0.000	155.000

CASE 4 ACCEL 58.8 RAD/SEC2, OMEG=0

WITH FRICTION, BEARINGS PERFECTLY ALIGNED

FY1	FX1	MZ1	FY2	FX2	FZ2
0.000	-122.635	-13.796	0.000	348.258	0.000
MZ2	FV3	FX3	FW3	MV3	MX3
-45.657	0.000	225.623	0.000	0.000	0.000
MW3	FY4	FX4	FZ4	MY4	MX4
21.118	54.484	-426.183	-75.613	-129.852	0.000
MZ4	FV5	FX5	FW5	MV5	MX5
-109.077	-9.184	-200.560	0.000	0.000	0.000
MW5	FY6	FX6	FZ6	MZ6	FV7
-43.848	9.116	217.589	-221.237	-175.025	0.000
FX7	FW7	MV7	FV8	FX8	FW8
-130.833	0.000	0.000	0.000	356.456	0.000
MV8	FY9	FX9	MZ9	T	
0.000	-.357	-17.029	-5.210	503.764	

WITH FRICTION, BEARINGS MISALIGNED

FY1	FX1	MZ1	FY2	FX2	FZ2
-47.224	-167.853	-19.617	215.528	467.893	133.356
MZ2	FV3	FX3	FW3	MV3	MX3
-67.536	200.624	300.040	76.554	-32.839	-22.772
MW3	FY4	FX4	FZ4	MY4	MX4
23.885	-383.774	-550.605	-114.683	-168.727	-82.552
MZ4	FV5	FX5	FW5	MV5	MX5
-134.245	-238.274	-250.566	171.122	75.082	72.591
MW5	FY6	FX6	FZ6	MZ6	FV7
-53.390	303.356	268.179	-315.523	-278.466	53.874
FX7	FW7	MV7	FV8	FX8	FW8
-172.456	-50.072	-16.419	146.751	472.496	126.626
MV8	FY9	FX9	MZ9	T	
-16.419	-24.644	-17.614	-9.266	664.127	

STOP
CP: 22.7 SEC I/O: 30.7 SEC

READY

READY
RUN:NUTRØD CASE IVA

NUTRØD 10:23 WEDNESDAY 07/01/70

NUTATING RØD FORCE ANALYSIS

CASE 4 ACCEL 58.8 RAD/SEC2, ØMEG=15.7 RAD/SEC

LZ2	LZ3	LZ7	LZ8	LR	LB
6.300	9.693	8.413	9.243	6.250	5.375

LZ5	LZ6	LD
32.700	30.850	15.500

LY3	LY5	LY7	LY8	LØD	WTD
1.880	1.880	2.170	2.450	0.670	250.000

FVB	FWB	MXB	FYD	FXD	FZD	MZD
-38.400	88.500	149.000	0.000	107.000	-26.000	-155.000

MU1	MU2	MU6	MU9	MU3	MU5	MU4
0.300	0.300	0.700	0.700	0.300	0.700	0.300

MUB3	MUB5	MU7	MU8
0.300	0.700	0.300	0.300

R1	R2	R6	R9	R3	R5
0.375	0.437	0.437	0.437	0.312	0.312

RØ4	RI4	RB3	RB5	R78	RT6
1.000	0.687	0.500	0.500	0.312	0.700

ZERØ FRICTIØN LØADS

FY1	FX1	MZ1	FY2	FX2	FZ2
0.000	-44.443	0.000	0.000	126.890	0.000

MZ2	FV3	FX3	FW3	MV3	MX3
0.000	0.000	82.447	0.000	0.000	0.000

MW3	FY4	FX4	FZ4	MY4	MX4
0.000	54.484	-164.894	-75.613	0.000	0.000

MZ4	FV5	FX5	FW5	MV5	MX5
0.000	-9.184	-82.447	0.000	0.000	0.000

MW5	FY6	FX6	FZ6	MZ6	FV7
0.000	9.116	39.060	-221.237	0.000	0.000

FX7	FW7	MV7	FV8	FX8	FW8
-45.000	0.000	0.000	0.000	127.446	0.000

MV8	FY9	FX9	MZ9	T
0.000	-.357	-63.614	0.000	155.000

CASE 4 ACCEL 58.8 RAD/SEC2, ØMEG=15.7 RAD/SEC

WITH FRICTIØN, BEARINGS PERFECTLY ALIGNED

FY1	FX1	MZ1	FY2	FX2	FZ2
0.000	-122.643	-13.797	0.000	348.278	0.000
MZ2	FV3	FX3	FW3	MV3	MX3
-45.712	0.000	225.635	0.000	0.000	0.000
MW3	FY4	FX4	FZ4	MY4	MX4
21.153	54.484	-426.201	-75.613	-129.857	0.000
MZ4	FV5	FX5	FW5	MV5	MX5
-109.190	-9.184	-200.565	0.000	0.000	0.000
MW5	FY6	FX6	FZ6	MZ6	FV7
-43.920	9.116	163.834	-221.237	-158.658	0.000
FX7	FW7	MV7	FV8	FX8	FW8
-130.852	0.000	0.000	P 0.000	356.487	0.000
MV8	FY9	FX9	MZ9	T	
0.000	-.357	-70.269	-21.520	503.876	

WITH FRICTIØN, BEARINGS MISALIGNED

FY1	FX1	MZ1	FY2	FX2	FZ2
-47.866	-170.128	-19.882	218.458	474.231	135.165
MZ2	FV3	FX3	FW3	MV3	MX3
-68.529	203.349	304.103	77.592	-33.283	-23.082
MW3	FY4	FX4	FZ4	MY4	MX4
24.247	-389.725	-558.066	-115.254	-170.953	-83.761
MZ4	FV5	FX5	FW5	MV5	MX5
-136.165	-241.395	-253.963	173.405	76.095	73.547
MW5	FY6	FX6	FZ6	MZ6	FV7
-54.189	307.346	217.982	-316.762	-270.608	54.607
FX7	FW7	MV7	FV8	FX8	FW8
-174.806	-50.751	-16.642	148.742	478.909	128.343
MV8	FY9	FX9	MZ9	T	
-16.642	-24.970	-71.018	-23.055	673.238	

STØP
CP: 22.4 SEC I/Ø: 36.3 SEC

READY

NUTRØD 10:08 WEDNESDAY 07/01/70

NUTATING RØD FØRCE ANALYSIS

CASE2 DECEL 118 RAD/SEC2, ØMEG=15.7 RAD/SEC

LZ2	LZ3	LZ7	LZ8	LR	LB
6.300	9.693	8.413	9.243	6.250	5.375

LZ5	LZ6	LD
32.700	30.850	15.500

LY3	LY5	LY7	LY8	LØD	WTD
1.880	1.880	2.170	0.450	0.670	250.000

FVB	FWB	MXB	FYD	FXD	FZD	MZD
-38.400	88.500	149.000	0.000	107.000	-26.000	310.000

MU1	MU2	MU6	MU9	MU3	MU5	MU4
0.300	0.300	0.700	0.700	0.300	0.700	0.300

MUB3	MUB5	MU7	MU8
0.300	0.700	0.300	0.300

R1	R2	R6	R9	R3	R5
0.375	0.437	0.437	0.437	0.312	0.312

RØ4	RI4	RB3	RB5	R78	RT6
1.000	0.687	0.500	0.500	0.312	0.700

ZERØ FRICTION LØADS

FY1	FX1	MZ1	FY2	FX2	FZ2
0.000	88.886	0.000	0.000	-253.780	0.000

MZ2	FV3	FX3	FW3	MV3	MX3
0.000	0.000	-164.894	0.000	0.000	0.000

MW3	FY4	FX4	FZ4	MY4	MX4
0.000	54.484	329.787	-75.613	0.000	0.000

MZ4	FV5	FX5	FW5	MV5	MX5
0.000	-9.184	164.894	0.000	0.000	0.000

MW5	FY6	FX6	FZ6	MZ6	FV7
0.000	9.116	-223.113	-221.237	0.000	0.000

FX7	FW7	MV7	FV8	FX8	FW8
89.999	0.000	0.000	0.000	-254.893	0.000

MV8	FY9	FX9	MZ9	T
0.000	-.357	-48.781	0.000	-310.000

CASE2 DECEL 118 RAD/SEC2, ØMEG=15.7 RAD/SEC

WITH FRICTION, BEARINGS PERFECTLY ALIGNED

FY1	FX1	MZ1	FY2	FX2	FZ2
0.000	32.963	-3.708	0.000	-94.628	0.000
MZ2	FV3	FX3	FW3	MV3	MX3
-12.420	0.000	-61.665	0.000	0.000	0.000
MW3	FY4	FX4	FZ4	MY4	MX4
5.781	54.484	132.064	-75.613	-45.654	0.000
MZ4	FV5	FX5	FW5	MV5	MX5
-36.745	-9.184	70.399	0.000	0.000	0.000
MW5	FY6	FX6	FZ6	MZ6	FV7
-15.530	9.116	-123.103	-221.237	-146.210	0.000
FX7	FW7	MV7	FV8	FX8	FW8
31.552	0.000	0.000	0.000	-93.217	0.000
MV8	FY9	FX9	MZ9	T	
0.000	-.357	-54.296	-16.629	-94.289	

WITH FRICTION, BEARINGS MISALIGNED

FY1	FX1	MZ1	FY2	FX2	FZ2
-7.852	28.036	-3.275	36.476	-82.082	23.264
MZ2	FV3	FX3	FW3	MV3	MX3
-11.789	34.297	-54.046	13.577	-5.910	-3.912
MW3	FY4	FX4	FZ4	MY4	MX4
4.243	-24.496	120.009	-72.073	-41.996	-15.689
MZ4	FV5	FX5	FW5	MV5	MX5
-31.034	-49.144	65.963	40.709	19.181	15.791
MW5	FY6	FX6	FZ6	MZ6	FV7
-12.722	64.635	-118.966	-248.042	-163.004	8.795
FX7	FW7	MV7	FV8	FX8	FW8
27.954	-8.834	-2.955	25.502	-82.000	22.411
MV8	FY9	FX9	MZ9	T	
-2.955	-5.522	-53.997	-16.623	-84.274	

STØP
CP: 18.8 SEC I/Ø: 34.2 SEC

READY

NUTATING ROD FORCE ANALYSIS

CASE 2 DECEL 118 RAD/SEC2, OMEG=0 RAD/SEC

LZ2	LZ3	LZ7	LZ8	LR	LB
6.300	9.693	8.413	9.243	6.250	5.375

LZ5	LZ6	LD
32.700	30.850	15.500

LY3	LY5	LY7	LY8	LOD	WTD
1.880	1.880	2.170	0.450	0.670	250.000

FVB	FWB	MXB	FYD	FXD	FZD	MZD
-38.400	88.500	149.000	0.000	0.000	-26.000	310.000

MU1	MU2	MU6	MU9	MU3	MU5
0.300	0.300	0.700	0.700	0.300	0.700

MUC4	MUI4	MUB3	MUB5	MU78	MUT6
0.300	0.300	0.300	0.700	0.300	0.700

R1	R2	R6	R9	R3	R5
0.375	0.437	0.437	0.437	0.312	0.312

R04	RI4	RB3	RB5	R78	RT6
1.000	0.687	0.500	0.500	0.312	0.700

ZERO FRICTION LOADS

FY1	FX1	MZ1	FY2	FX2	FZ2
0.000	88.886	0.000	0.000	-253.780	0.000

MZ2	FV3	FX3	FW3	MV3	MX3
0.000	0.000	-164.894	0.000	0.000	0.000

MW3	FY4	FX4	FZ4	MY4	MX4
0.000	54.484	329.787	-75.613	0.000	0.000

MZ4	FV5	FX5	FW5	MV5	MX5
0.000	-9.184	164.894	0.000	0.000	0.000

MW5	FY6	FX6	FZ6	MZ6	FV7
0.000	9.116	-169.352	-221.237	0.000	0.000

FX7	FW7	MV7	FV8	FX8	FW8
89.999	0.000	0.000	0.000	-254.893	0.000

MV8	FY9	FX9	MZ9	T
0.000	-.357	4.459	0.000	-310.000

CASE 2 DECEL 118 RAD/SEC2, OMEG=0 RAD/SEC

WITH FRICTION, BEARINGS PERFECTLY ALIGNED

FY1	FX1	MZ1	FY2	FX2	FZ2
0.000	39.541	-4.448	0.000	-113.511	0.000
MZ2	FV3	FX3	FW3	MV3	MX3
-14.881	0.000	-73.970	0.000	0.000	0.000
MW3	FY4	FX4	FZ4	MY4	MX4
6.924	54.484	158.038	-75.613	-52.559	0.000
MZ4	FV5	FX5	FW5	MV5	MX5
-43.203	-9.184	84.069	0.000	0.000	0.000
MW5	FY6	FX6	FZ6	MZ6	FV7
-18.470	9.116	-83.861	-221.237	-134.210	0.000
FX7	FW7	MV7	FV8	FX8	FW8
37.853	0.000	0.000	0.000	-111.822	0.000
MV8	FY9	FX9	MZ9	T	
0.000	-.357	-.208	-.126	-113.131	

WITH FRICTION, BEARINGS MISALIGNED

FY1	FX1	MZ1	FY2	FX2	FZ2
-9.205	32.865	-3.840	42.762	-96.219	27.272
MZ2	FV3	FX3	FW3	MV3	MX3
-13.804	40.206	-63.355	15.915	-6.928	-4.586
MW3	FY4	FX4	FZ4	MY4	MX4
4.966	-37.566	140.318	-72.037	-47.319	-16.744
MZ4	FV5	FX5	FW5	MV5	MX5
-35.512	-55.688	76.963	47.014	22.317	18.034
MW5	FY6	FX6	FZ6	MZ6	FV7
-14.668	73.580	-76.982	-252.086	-156.097	10.311
FX7	FW7	MV7	FV8	FX8	FW8
32.772	-10.356	-3.464	29.895	-96.126	26.271
MV8	FY9	FX9	MZ9	T	
-3.464	-6.329	0.019	-1.936	-98.812	

STOP
CP: 18.7 SEC I/O: 25.9 SEC

READY

APPENDIX B

CONTACT ANGLE OPTIMIZATION FOR THRUST BEARINGS 2 AND 6

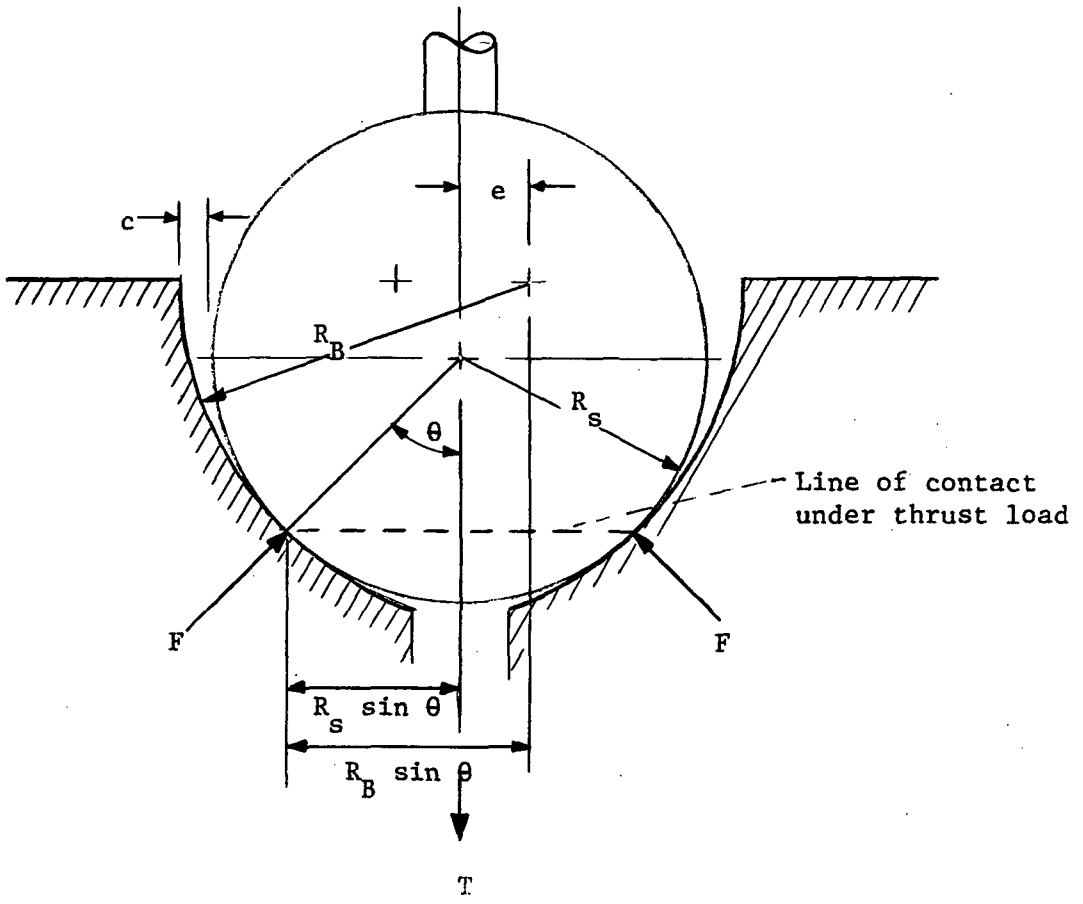

The line of contact under thrust load is a circle whose circumference is

$$C_T = 2\pi R_s \sin \theta$$

The normal reaction load per unit length of contact is F. Summing forces in the direction of thrust load gives:

$$T = C_T F \cos \theta = (2\pi R_s \sin \theta)(F \cos \theta) = \pi R_s F \sin 2\theta$$

or

$$F = \frac{T}{\pi R_s \sin 2\theta}$$

Therefore, for a given T and R_s, F is a minimum when $\theta = \pi/4$. Also from the above figure,

$$R_B = R_s + C + e$$

and

$$R_B \sin \theta = R_s \sin \theta + e$$

Therefore,

$$\sin \theta = \frac{e}{C + e}$$

So, for a specified angle θ and clearance C, eccentricity e is fixed.

REFERENCES

1. Krasner, Morton H.; Davison, Harry W.; and Diaguila, Anthony J.: Conceptual Design of a Compact Fast Reactor for Space Power. NASA TM X-67859, 1971.

2. Kurzeka, W. J.: Development of Bearings for Nuclear Reactors in Space. Proceedings of the third Aerospace Mechanism Symposium. Rep. TM-33-382, Jet Propulsion Lab., California Inst. Tech. (NASA CR-97758), Oct. 1, 1968, pp. 85-91.

3. Balkwill, J. K.: Mechanical Elements Operating in Sodium and Other Alkali Metals. Vol. 1 - Literature Survey. Rep. LMEC 68-5, vol. 1, Atomics International, 1968.

4. Gluyas, R. E.; and Lietzke, A. F.: Materials Technology Program for a Compact Fast Reactor for Space Power. NASA TM X-67869, 1971.

TABLE I. - SUMMARY OF LOAD ANALYSES

Base case	Acceleration rate, rad/sec^2	Deceleration rate, rad/sec^2	Maximum velocity rad/sec	Angle at maximum velocity, deg	Cermet friction coefficient	Graphite friction coefficient
I	49.1	196.4	15.7	144	0.3	0.3
II	49.1	196.4	15.7	144	.7	.3
III	58.8	118.0	15.7	120	.3	.3
IV	58.8	118.0	15.7	120	.7	.3

For each above "Base case" the following variations were analyzed.

A. Acceleration and deceleration torque supplied by an actuator attached to the penetration device input shaft.

B. Acceleration torque supplied by constant force spring attached to the penetration device input shaft. The force provided by the accelerating spring is assumed to be applied throughout the scram cycle. Deceleration torque supplied by a dashpot located within the reactor and located:

1. Above control drum in-phase with crank arm

2. Above control drum out-of-phase with crank arm

3. Below control drum in-phase with crank arm

4. Below control drum out-of-phase with crank arm

TABLE II. - CERMET BEARING MATERIAL PROPERTIES FOR BEARING DESIGN

Property	Assumed design value
Compression strength	30 000 psi
Tensile strength	10 000 psi
Shear strength	10 000 psi
Creep	Negligible
Modulus of elasticity	5×10^7 psi
Poisson ratio	0.22
Friction coefficient	0.3 to 0.7
Wear rate	10^{-10} in.^{3}/in. #
Thermal expansion	3.5×10^{-6} to 4.0×10^{-6}/$^\circ$F
Conductivity	10 Btu/(hr)(ft)($^\circ$F)
Specific heat	0.06 Btu/(lb)($^\circ$F)
Density	8 gm/cc
Sinter temperature	4000° F
Maximum particle size	100 micron

TABLE III. - GRAPHITE BEARING MATERIAL PROPERTIES FOR BEARING DESIGN

Property	70° F	2200° F
Compression strength	20 000 psi	20 000 psi
Tensile strength	10 000 psi	10 000 psi
Modulus of elasticity	1.68×10^6 psi	1.96×10^6 psi
Poisson's ratio	0.15	0.20
Coefficient of thermal expansion	3.7×10^{-6} in./in. $^\circ$F	4.5×10^{-6} in./in. $^\circ$F
Thermal conductivity	68 Btu/(hr)(ft)($^\circ$F)	18 Btu/(hr)(ft)($^\circ$F)
Apparent density	1.80 to 1.88 gms/cc	
Maximum particle size	0.001 in.	

TABLE IV. - EFFECT OF DASHPOT LOCATION ON CONTROL DRUM BEARING RADIAL LOADS

[Cases IB1 through 4 and IIB1 through 4 at ω = 15.7 rad/sec; α_{accel} = 49.1 rad/sec^2; α_{decel} = 196.4 rad/sec^2; t = 0.32 sec; θ_c = 144°]

Case	IB1	IIB1	IB2	IIB2	IB3	IIB3	IB4	IIB4
Dashpot location	Above control drum				Below control drum			
Dashpot angle[a]	0		180°		0		180°	
Friction coefficient	0.3	0.7	0.3	0.7	0.3	0.7	0.3	0.7
Bearing 5								
Load (lb) accel	102	157	102	157	103	157	103	157
Load (lb) decel	102	157	102	157	103	157	103	157
Load reversal	No	No	No	No	No	No	No	No
Bearing 6								
Load (lb) accel	60	118	60	118	63	121	63	121
Load (lb) decel	89	144	30	89	-302	-238	422	451
Load reversal	No	No	No	No	Yes	Yes	No	No
Bearing 9								
Load (lb) accel	65	68	65	68	67	71	67	71
Load (lb) decel	475	437	-360	-333	96	99	39	45
Load reversal	No	No	Yes	Yes	No	No	No	No

[a]"Dashpot angle" indicates the angle between the vane of the dashpot and the penetration device crank arm.

TABLE V. - EFFECT OF DASHPOT LOCATION ON CONTROL DRUM BEARING RADIAL LOADS

[Cases IIIB1 through 4 and IVB1 through 4 at ω = 15.7 rad/sec; α_{accel} = 58.8 rad/sec^2; α_{decel} = 118.0 rad/sec^2; t = 0.267 sec; θ_c = 120°]

Case	IIIB1	IVB1	IIIB2	IVB2	IIIB3	IVB3	IIIB4	IVB4
Dashpot location	Above control drum				Below control drum			
Dashpot angle[a]	0		180°		0		180°	
Friction coefficient	0.3	0.7	0.3	0.7	0.3	0.7	0.3	0.7
Bearing 5								
Load (lb) accel	117	174	117	174	117	175	117	175
Load (lb) decel	117	174	117	174	117	175	117	175
Load reversal	No	No	No	No	No	No	No	No
Bearing 6								
Load (lb) accel	76	136	76	136	79	139	79	139
Load (lb) decel	97	155	54	115	-188	-135	338	376
Load reversal	No	No	No	No	Yes	Yes	No	No
Bearing 9								
Load (lb) accel	66	69	66	69	68	71	68	71
Load (lb) decel	361	335	-243	-227	89	92	48	53
Load reversal	No	No	Yes	Yes	No	No	No	No

[a]See footnote table IV.

TABLE VI. - SUMMARY OF BEARING DESIGN LOADS

Bearing number	Maximum radial load, lb	Maximum thrust load, lb
1	177	0
2	522	140
3	314	0
4	340	0
5	350	0
6	500	250
7	181	0
8	495	0
9	75	0

TABLE VII. - SUMMARY OF BEARING DESIGNS

Bearing number	Type[a]	Design load, lb	Diameter, in.	Length, in.	R_c or e,[b] in.	Radial clearance, in.$\times 10^3$	Maximum compressive stress, psi	Maximum contact angle, deg	Tolerable misalinement	
									Axial, in.	Angular, rad
1	CJ	177	1.00	0.75	40	1.0 to 1.5	3 000	80.5	0.191	0.0048
2	JT	522	1.40	NA	0.0015 to 0.0038	1.0 to 1.5	2 380	NA	NA	NA
3	CJ	314	0.75	0.75	40	1.0 to 1.5	4 940	104.0	0.181	0.0045
4	CJ	340	0.50	0.60	40	1.0 to 1.5	6 520	106.0	.072	.0018
5	CJ	350	1.20	.75	125	2.0 to 2.5	13 730	64.8	.185	.0015
6	JT	500	2.00	NA	0.005 to 0.006	2.0 to 2.5	10 534	NA	NA	NA
7	CJ	181	.625	.75	40	1.0 to 1.5	3 900	81.6	0.219	0.0055
8	CJ	495	.625	.75	40	1.0 to 1.5	6 280	117.4	.139	.0035
9	CJ	75	1.200	1.00	40	2.0 to 2.5	11 930	16.8	.458	.011

[a] CJ = crowned journal bearing
JT = spherical journal thrust bearing

[b] R_c = crown radius for CJ
e = ellipticity for JT

TABLE VIII. - COMPARISON OF RESULTANT RADIAL LOADS (POUNDS) FOR ORIGINAL AND FINAL DESIGN BEARING CONFIGURATION

[α = 58.8 rad/sec^2; ω = 15.7 rad/sec; μ_{cermet} = 0.7; μ_{carbon} = 0.3]

Bearing number	Original design	Final design
1	177	137
2	522	405
3	314	284
4	680	540
5	350	279
6	377	292
7	181	143
8	495	390
9	75	71

TABLE IX. - SUMMARY OF JOINT DESIGNS GRAPHITE IN T-111

Bearing number	Fit diameter, in.	Diametrical interference, mils	Maximum stress graphite, psi		Maximum stress T-111, psi		Minimum torque resistant at 450°F,[a] in.-lb	Maximum bearing friction torque,[b] in.-lb
			Rt	2200°F	Rt	2200°F		
1	1.500	1-2	2990	6457	2962	6406	150	20
2	1.800	1-2	2423	5524	506	1154	310	68
3	1.250	1-2	4208	7950	2285	4315	294	33
4	.900	0.5-1.5	1434	8450	1053	6208	54	86
7&8	1.125	1-2	4446	8512	4365	8358	462	16

[a]Based upon a coefficient of friction between the graphite and T-111 equal to 0.30.

[b]Based upon a coefficient of friction in the bearing of 0.30.

TABLE X. - SUMMARY OF CLAMPING LOADS AND STRESSES JOURNALS 6 AND 9

	Journal 6		Journal 9	
α(cermet), in./in.-^{o}F	3.5×10^{-6}	4.0×10^{-6}	3.5×10^{-6}	4.0×10^{-6}
Shaft diameter, in.	0.875		0.8125	
Clamp tube o.d., in.	1.250		1.150	
Clamp tube length, in.	2.75		2.00	
Clamp force, lb:				
R.T.	0	0	0	0
450^{o} F	900	1590	560	992
2200^{o} F	489	2930	483	2900
Cermet stress, psi:				
450^{o} F	498	882	915	1620
2200^{o} F	271	1630	789	4730
Maximum shaft stress, psi:				
450^{o} F	2930	5180	1510	2670
2200^{o} F	1590	9650	1300	7810
Clamp tube stress, psi:				
450^{o} F	1440	2540	1070	1910
2200^{o} F	781	2930	929	5570

TABLE XI. - SUMMARY OF AXIAL CLAMP DESIGN FOR CERMET JOURNAL NUMBER 5

Coefficient of thermal expansion of cermet, in./in.-°F×10⁶	Initial interference, mils ±0.1	Minimum axial clamping force, lb			Stress, ksi								
					Post			Sleeve			Cermet		
		R.T.	450° F	2200° F	R.T.	450° F	2200° F	R.T.	450° F	2200° F	R.T.	450° F	2200° F
3.5	1.2	1820	1620	630	10.9	9.8	4.9	8.8	7.9	3.9	2.3	2.0	1.0
3.6	1.0	1490	1220	560	9.3	8.5	4.5	7.4	6.8	3.6	1.9	1.7	.9
3.7	.9	1320	1200	660	8.4	7.8	5.1	6.7	6.3	4.0	1.7	2.6	1.1
3.8	.7	990	920	600	6.8	6.4	4.8	5.4	5.1	3.8	1.4	1.3	1.0
3.9	.6	830	810	690	5.9	5.8	5.2	4.7	4.6	4.2	1.2	1.2	1.1
3.95	.5	830	810	690	5.9	5.8	5.2	4.7	4.6	4.2	1.2	1.2	1.1
4.0	.4	490	500	630	4.2	4.3	4.9	3.3	3.4	3.9	.9	.9	1.0

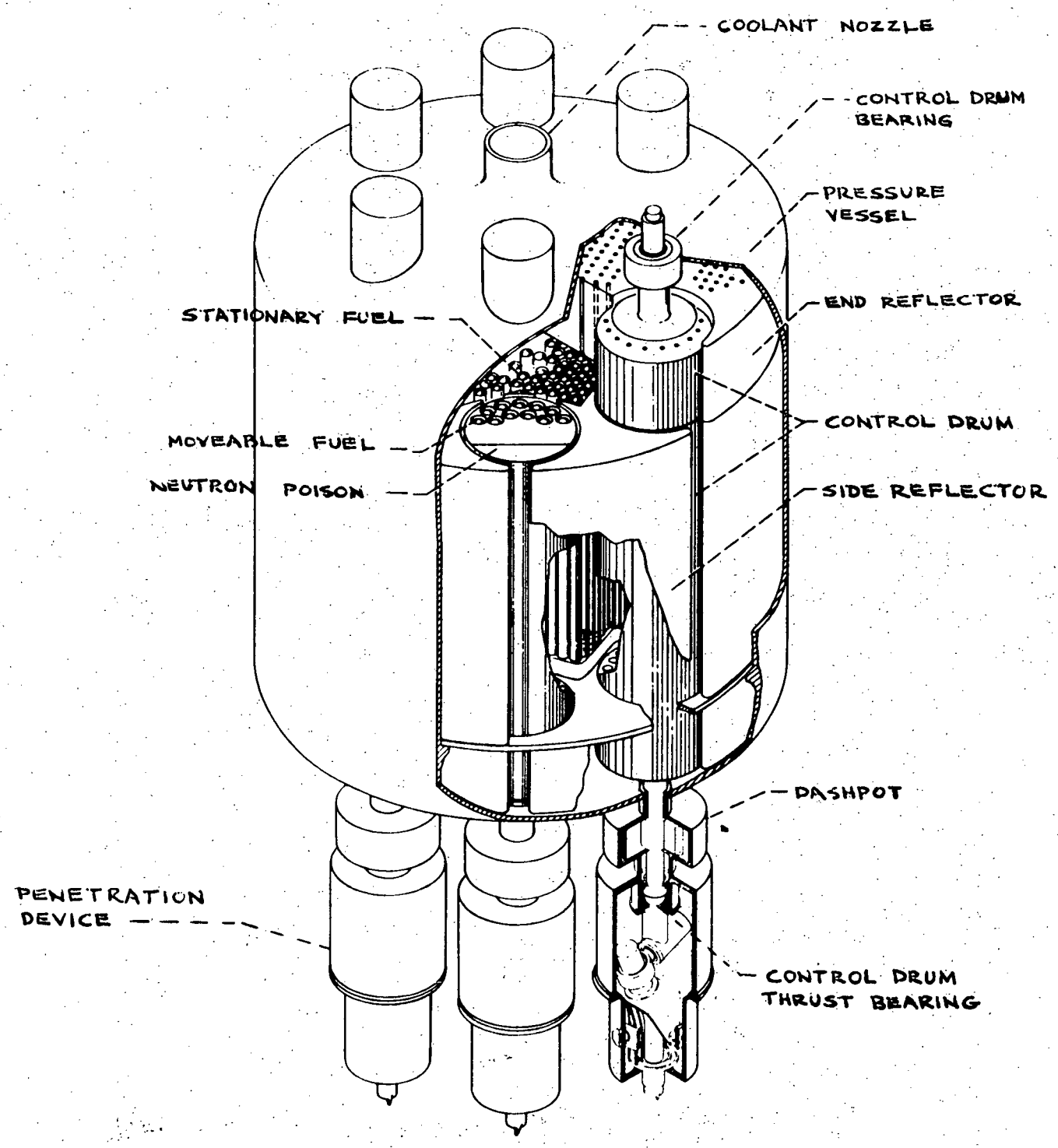

FIGURE 1. COMPACT FAST REACTOR - REFERENCE DESIGN

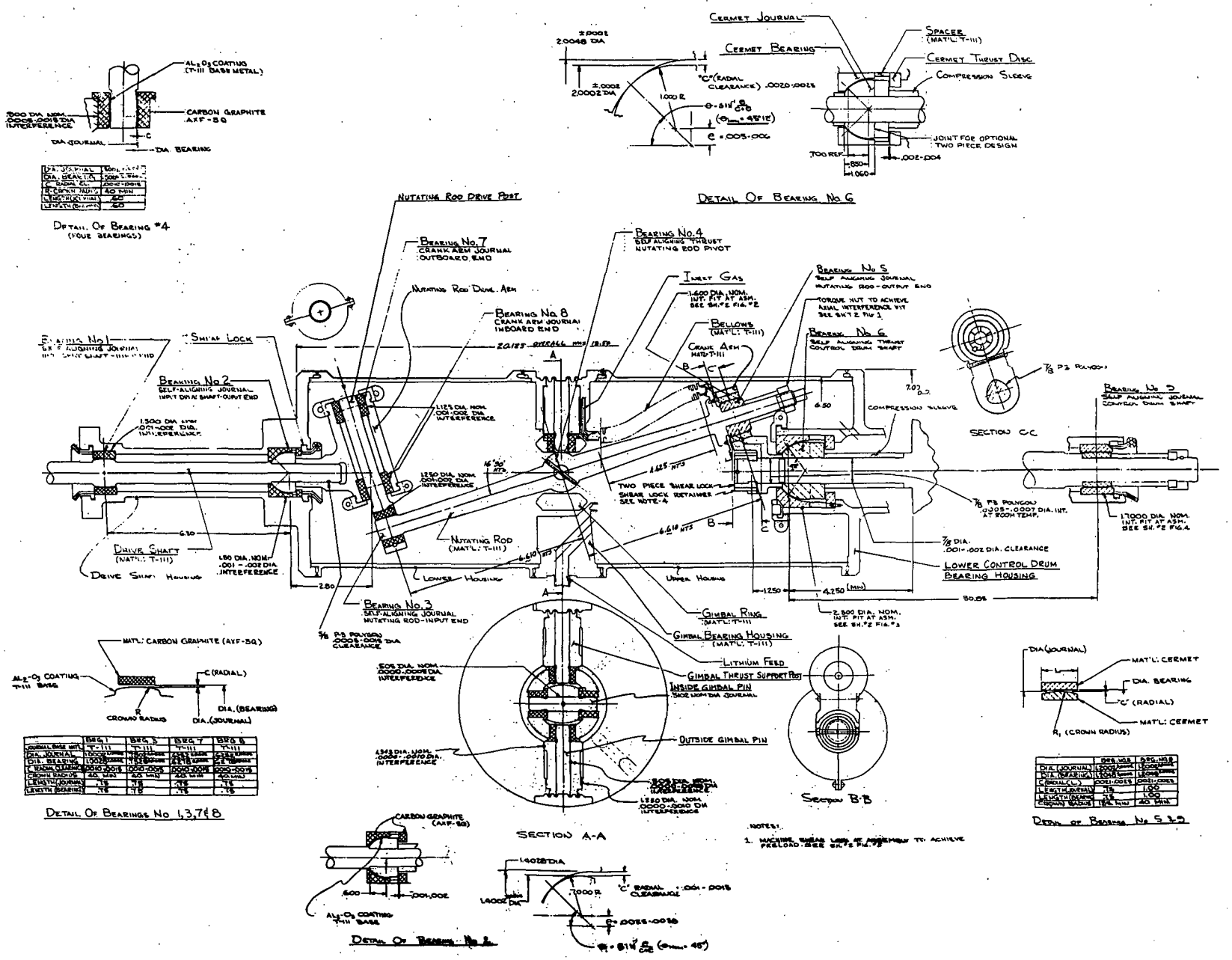

Fig. 2 Penetration Device

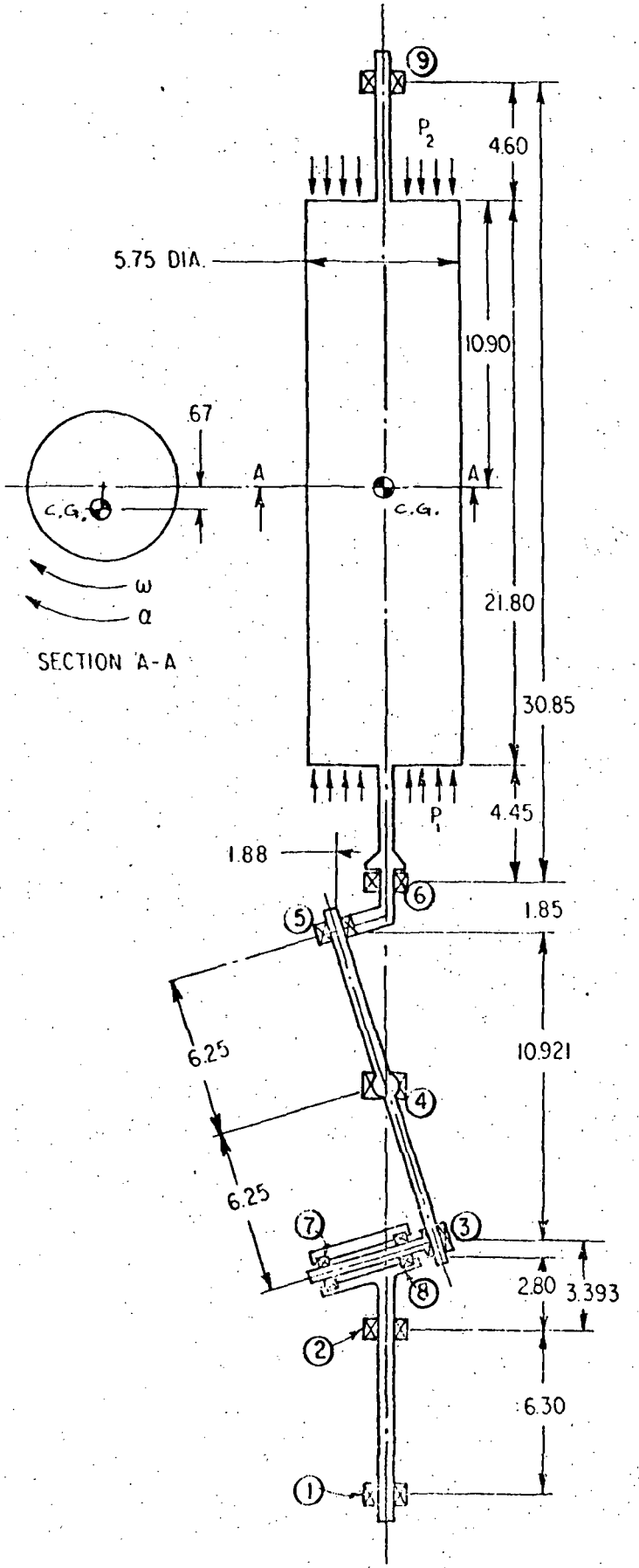

CONTROL DRUM:

WEIGHT = 250. LBS

$I = 0.22$ LB-SEC^2-FT

ω(MAX) = 15.7 RAD/SEC

α(MAX) = 49.1 RAD/SEC^2

α(MIN) = -196.4 RAD/SEC^2

$P_1 - P_2$ = 1.0 PSI

Fig. 3 Control Drum and Penetration Device Schematic

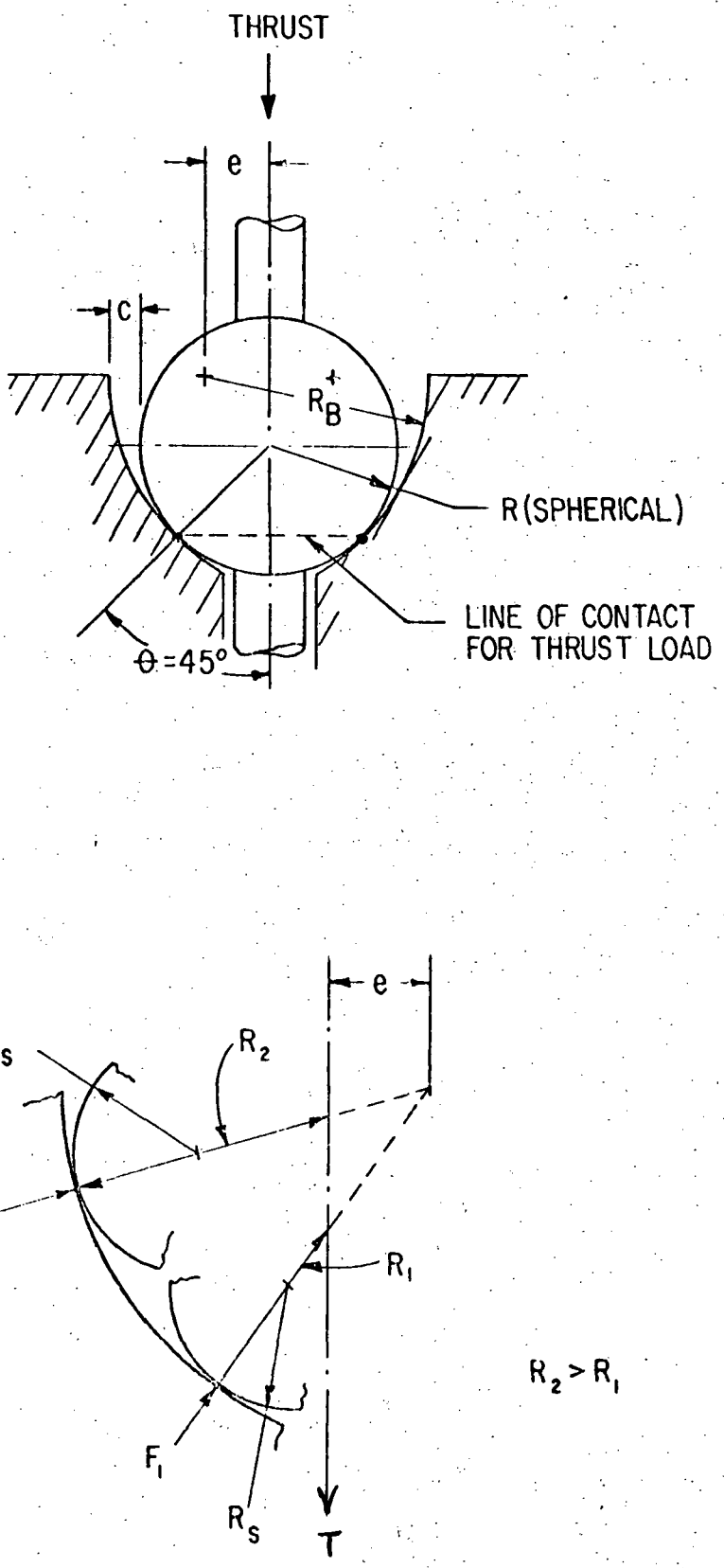

Fig. 4 Combined Journal and Thrust Bearing

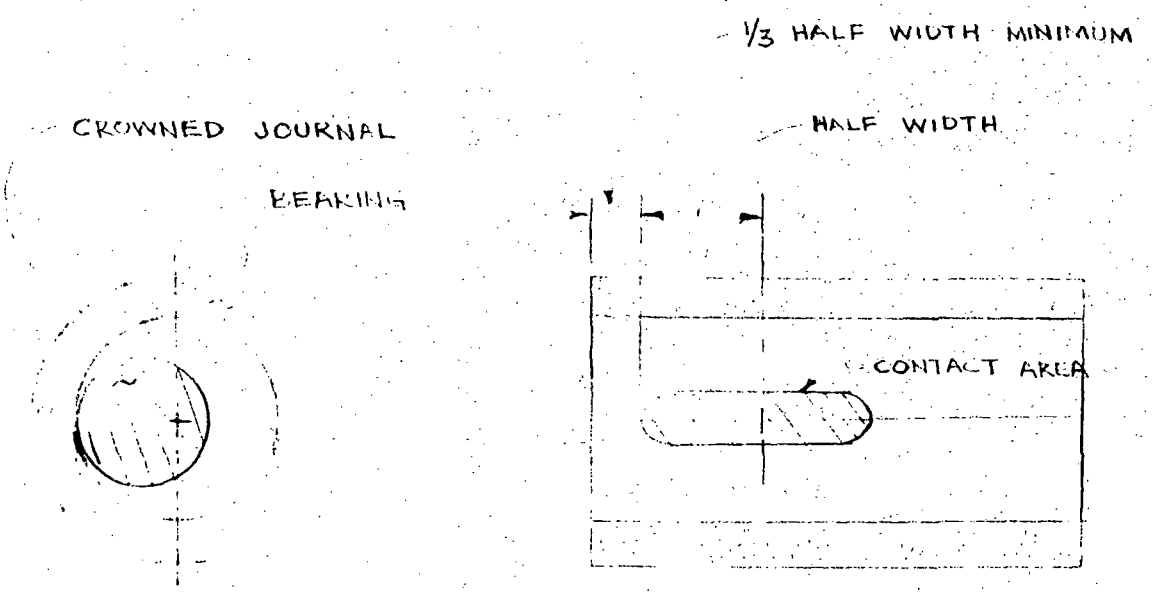

Fig. 5 HERTZIAN CONTACT AREA

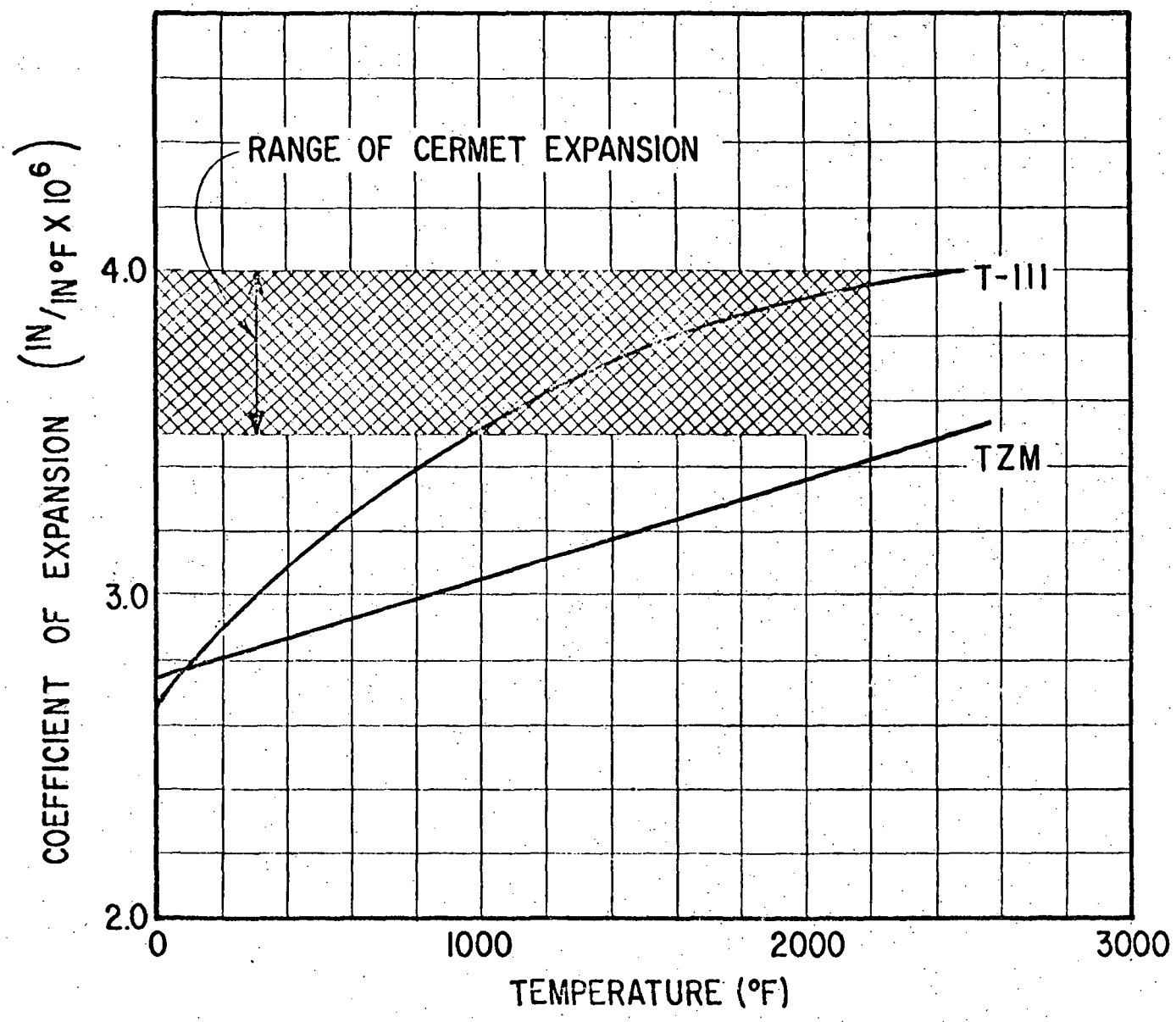

Fig. 6 Linear Coefficient of Thermal Expansion of TZM, T-111 and Cermet Materials. Average Rate From 20°F to Temperature Indicated

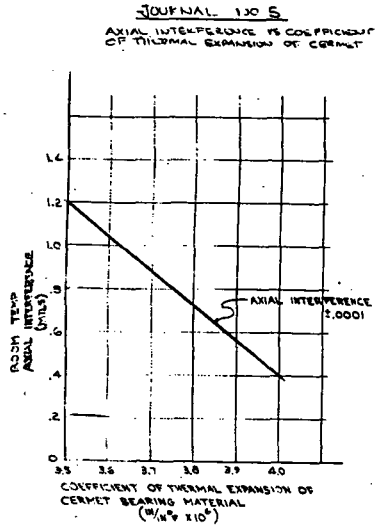

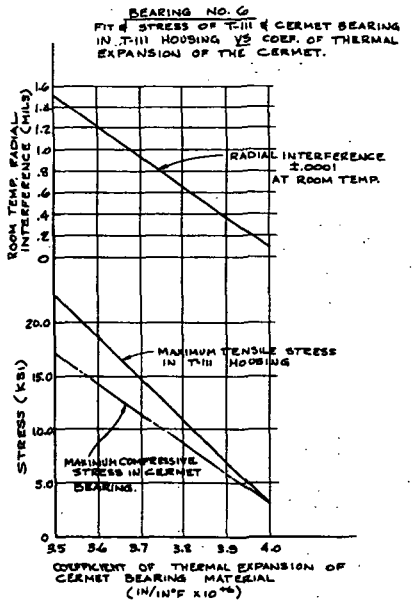

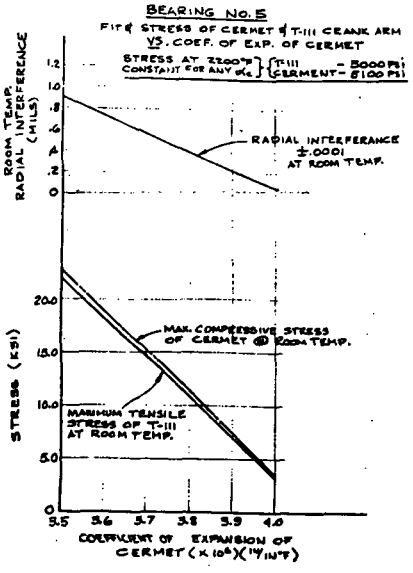

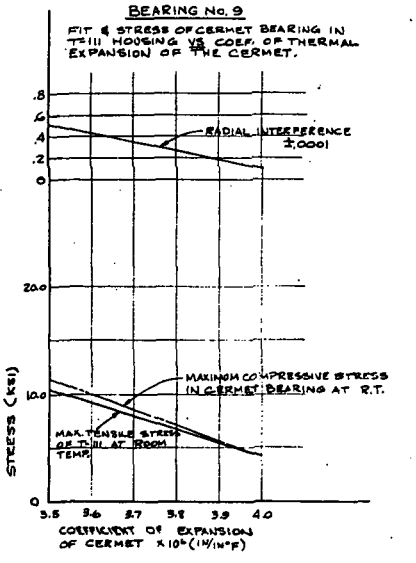

FIG. 7 Initial interference fits for cermet bearing components over the assumed range of thermal expansion coefficients.

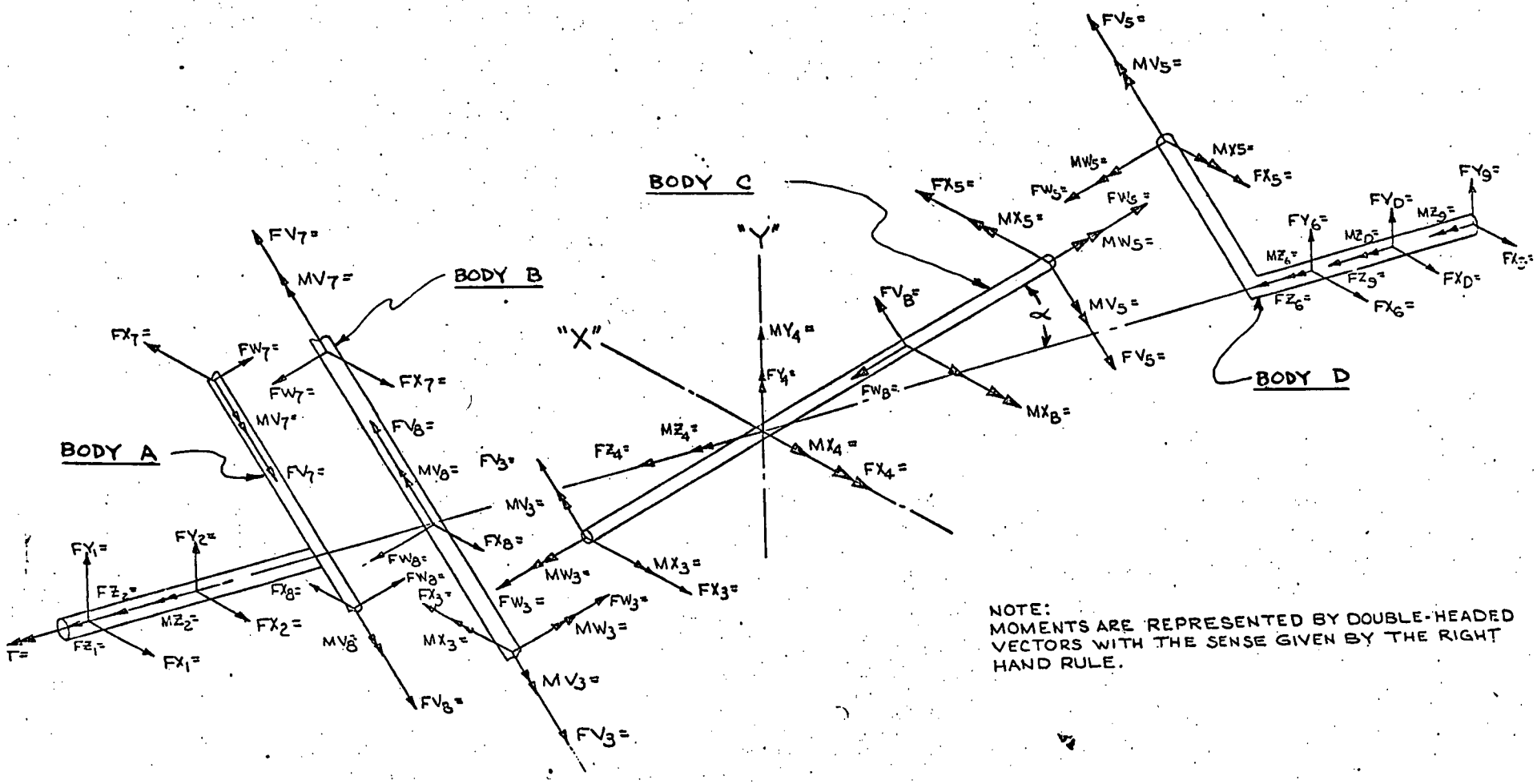

FIG. 8 PENETRATION DEVICE FREE BODY DIAGRAM